

# Mediator Decay through mixing with Degenerate Spectrum

Ayuki Kamada<sup>a</sup>, Takumi Kuwahara<sup>b</sup>, Shigeki Matsumoto<sup>c</sup>, Yu Watanabe<sup>c</sup>, and Yuki Watanabe<sup>c</sup>

<sup>a</sup> *Institute of Theoretical Physics, Faculty of Physics, University of Warsaw, ul. Pasteura 5, PL-02-093 Warsaw, Poland*

<sup>b</sup> *Center for High Energy Physics, Peking University, Beijing 100871, China*

<sup>c</sup> *Kavli IPMU (WPI), UTIAS, University of Tokyo, Kashiwa, Chiba 277-8583, Japan*

## Abstract

The decay of the mediator particle into standard model (SM) particles plays a significant role in exploring the dark sector scenario. We consider such a decay, taking the dark photon mediator as an example that mixes with the SM photon. We find that it requires a careful analysis of the decay rate in the presence of an SM vector boson (e.g.,  $Z$  boson,  $\rho$  meson, and true muonium, etc.) nearly degenerate with the mediator particle in mass. The decay rate of the mediator particle calculated in the mass eigenstate basis **does not** agree with the correct result, given by the imaginary parts of the poles for the vector boson propagators, when the mixing parameter is smaller than a specific value. In such a case, the decay rate calculated by treating the mixing as a perturbative parameter is in agreement with the correct result. We clarify specific values for the mixing parameter quantitatively using several concrete examples of the SM vector bosons degenerate with the dark photon. When the mass mixing between the vector boson and dark photon is smaller (larger) than the decay width of the vector boson, the latter (former) method to calculate the decay rate of the mediator particle gives the correct result.

# 1 Introduction

Decay is one of the essential features of unstable particles. It plays a crucial role in particle physics for discovering new particles in terrestrial experiments and cosmological observations. Dark-sector models have been extensively studied among various new physics models over the last decade. The dark-sector particles are neutral under the standard model (SM) gauge symmetries, have their own gauge interactions, and are not directly coupled to the SM particles. Some dark-sector particles, referred to as mediator particles in this article, mix with the SM neutral particles, such as the photon, the neutral component of the SM Higgs boson, and the neutrino. When the mediator particle is lightest in the dark sector, it decays only into the SM particles through the mixing. Its decay provides promising signals to explore the dark sector, e.g., the impact on the cosmic history [1–5], and the visible (long-lived) decay signal at collider and fixed-target experiments [6–19].

The mass of the mediator particle is still unknown, and a wide range of the mass must be explored. In some cases, the mass of the mediator field could be very close to that of an SM neutral field, which is not necessarily the fundamental one but also a resonance or a bound state composed of the SM elementary particles. In this article, we refer to it as a degenerate partner. When the mediator mass is very close to that of the degenerate partner, the mediator field almost maximally mixes with the partner field. In such a case, we naïvely expect that both the decay widths of these mass eigenstates to the SM particles are comparable. On the other hand, as far as the mixing parameter is considered small, i.e., a perturbative one, the decay width of the mediator particle is expected to be suppressed by the mixing parameter. Hence, the width of the mediator particle becomes smaller than that of the degenerate partner. Since the two statements above seem incompatible, there must be a criterion to specify a parameter region where one statement is valid and the other is not.

The total decay width of the mediator particle is computed in several ways. One way is taking a mass basis, where the mixing among the fields is removed by redefining the fields (e.g., via the diagonalization of their mass matrix) and computing the decay width of the mediator(-like) particles in a standard perturbation manner. This method corresponds to the first statement mentioned above, which we refer to as the “classical” method in this article. In this method, the decay rates of both the mass eigenstates approach each other when they are nearly degenerate in mass. Meanwhile, when the mass mixing between them is treated as a perturbative one, the decay width of the mediator particle is computed by inserting the mass mixing into the decay amplitude: the mediator particle is converted into the degenerate partner by the insertion, and the partner decays into the SM particles. This method corresponds to the second statement mentioned above, which we refer to as the “mass-insertion” method. In this method, the mixing parameter suppresses the decay width of the mediator particle. Furthermore, when the mediator particle and the degenerate partner are nearly degenerate in mass, the decay width of the mediator particle is proportional to the inverse of the decay width of the degenerate partner. Finally, the third method is to compute the total decay width using the imaginary part of the propagator pole in some scattering amplitude involving the mediator particle as an intermediate state. Thanks to this method, we find that the “classical” (“mass-insertion”) method is validated as far as the mass mixing is larger (smaller) than the decay width of the degenerate partner. We also demonstrate in this article that our criterion works well using several concrete examples, where the validity of the approximation methods (the first two methods mentioned above) is quantitatively figured out by comparing with the rigorous method (the last method).

We take the dark photon model as a concrete example of the mediator field, which has a kinetic mixing with the SM photon [20]. The dark photon also mixes with various massive vector fields; we

consider the  $Z$  boson,  $\rho$  meson, and true muonium ( $\mu^+\mu^-$  bound state) as such a vector field (i.e., the degenerate partner), covering a wide range of mass and decay width. The physical dark photon decays into the SM particles by mixing with the SM photon and the massive vector fields.

This paper is organized as follows. In Section 2, we give a general discussion of the decay rate of the mediator particle by considering the dark photon model as a concrete example. We introduce three methods of computing the total decay rate mentioned above: the “classical” method, the “mass-insertion” method, and the decay rate given by the imaginary part of the propagator pole. There, we find the criteria for the validity of the “classical” and the “mass-insertion” methods. In Section 3, we discuss the decay of the dark photon in the presence of the concrete degenerate partner. We consider the  $Z$  boson, the  $\rho$  meson, and the true muonium as examples of the degenerate partner. In Section 4, we summarize our criteria for the total decay width of the mediator particle and apply it to other resonances not treated in Section 3. Section 5 is devoted to concluding our study.

## 2 Mediator particle decay

In this section, we calculate the decay of a mediator particle degenerate with some SM particle in mass. We consider the case with a vector mediator particle, i.e., the so-called dark photon model, which kinematically mixes with the SM photon (or hypercharge gauge boson). The Lagrangian of this dark photon model is given as follows:

$$\mathcal{L} = \mathcal{L}_{\text{SM}} + \mathcal{L}_{\text{DS}} - \frac{1}{4}F'_{\mu\nu}F'^{\mu\nu} + \frac{1}{2}\bar{m}_{A'}^2 A_\mu'^2 + \frac{\epsilon}{2\cos\theta_W}F'_{\mu\nu}B^{\mu\nu}. \quad (1)$$

Here,  $A'_\mu$  and  $F'_{\mu\nu}$  denote the dark photon field and its field strength tensor, respectively, while  $B_{\mu\nu}$  is the field strength tensor of the SM hypercharge gauge boson, with  $\theta_W$  being the Weinberg angle. The first two terms,  $\mathcal{L}_{\text{SM}}$  and  $\mathcal{L}_{\text{DS}}$ , are the Lagrangians of the SM sector and the dark sector, respectively. The dark photon couples not only to the SM photon but also to the  $Z$  boson after the electroweak symmetry is spontaneously broken. Moreover, the SM photon may mix with other massive SM vector bosons in the low-energy spectrum, such as hadronic vector resonances (e.g.,  $\rho, \omega, J/\psi$ , etc.) and other bound states (e.g., the positronium  $e^+e^-$ , the true muonium  $\mu^+\mu^-$ , etc.).

We now consider the system containing three vector fields: the SM photon  $A_\mu$ , the dark photon  $A'_\mu$ , and a massive SM vector boson (i.e., the degenerate partner)  $V_\mu$ . In the next section, we discuss several concrete examples of the vector boson  $V$ , such as the  $Z$  boson, the  $\rho$  meson, and the true muonium. The vector boson  $V$  may have a kinetic mixing with the dark photon  $A'$  from the first beginning. Even if no mixing between  $V$  and  $A'$  exists at the beginning, one can obtain such a kinetic mixing when one removes the kinetic mixing term between  $V$  and the SM photon  $A$  by shifting  $A$ . The field redefinition of the vector field  $V$  then absorbs the kinetic mixing between  $V$  and  $A'$ , and one obtains the mass mixing between the two fields. The mass matrix is generally written as

$$M_{V,A'}^2 = \bar{m}_V^2 \begin{pmatrix} 1 & -\eta \\ -\eta & \eta^2 + \delta^2 \end{pmatrix}, \quad (2)$$

where  $\bar{m}_V^2$  is the mass parameter of  $V$  in the interaction basis (with only the kinetic mixing between  $V$  and  $A'$ ). The off-diagonal component  $\eta$  arises from the kinetic mixing between  $A'$  and  $V$ , and  $\delta$  is

the mass ratio  $\bar{m}_{A'}/\bar{m}_V$ . We obtain the mass eigenvalues and the mixing angle as

$$\begin{aligned} m_{X,Y}^2 &= \frac{\bar{m}_V^2}{2} [1 + \eta^2 + \delta^2 \pm (1 - \eta^2 - \delta^2) \cos 2\theta \mp \eta \sin 2\theta] , \\ \tan 2\theta &= -\frac{2\eta}{1 - \eta^2 - \delta^2} . \end{aligned} \quad (3)$$

Here, the mass mixing angle  $\theta$  ranges from  $-\pi/4$  to  $\pi/4$  and  $m_{X,Y}^2$  gives the mass eigenvalues of  $V$  and  $A'$ , respectively, except for  $\delta$  being close to unity. Since the mass mixing angle  $\theta$  jumps from  $\mp\pi/4$  to  $\pm\pi/4$  (the sign depends on the sign of  $\eta$ ) at  $\delta \simeq 1$ , the mass eigenvalues have a mass gap of  $\eta$ . This raises a question of how we identify the particles near  $\delta \simeq 1$ . As we will see later, the decay rates of the mass eigenstates are identical at a certain  $\delta \simeq 1$ , and hence, the rates are smooth as a function of  $\delta$ , unlike the mass eigenvalues. We will identify the physical states of the particles  $V$  and  $A'$  by those whose decay rates at  $\delta \simeq 1$  are smoothly connected to their decay rates at  $\delta$  far from 1. As a result, the relation between the mass eigenstates and the particles  $V$  and  $A'$  interchanges twice around  $\delta \simeq 1$ .

Suppose  $V$  couples to  $f$  in the interaction basis as

$$\mathcal{L}_{\text{int}} = g_V V_\mu \bar{f} \gamma^\mu f + e Q_f A_\mu \bar{f} \gamma^\mu f . \quad (4)$$

Here,  $g_V$  and  $e$  are coupling constants, and  $Q_f$  is the electromagnetic charge of the fermion  $f$ . The mass basis for the vector fields relates to the interaction basis as follows:

$$\begin{pmatrix} A'_\mu \\ V_\mu \\ A_\mu \end{pmatrix}_{\text{int}} = C_{\text{kin}} \begin{pmatrix} \cos \theta & \sin \theta & 0 \\ -\sin \theta & \cos \theta & 0 \\ 0 & 0 & 1 \end{pmatrix} \begin{pmatrix} A'_\mu \\ V_\mu \\ A_\mu \end{pmatrix}_{\text{mass}} \equiv C \times \begin{pmatrix} A'_\mu \\ V_\mu \\ A_\mu \end{pmatrix}_{\text{mass}} . \quad (5)$$

Here,  $C_{\text{kin}}$  is the mixing matrix for diagonalizing (canonicalizing) the kinetic terms and depends on the kinetic mixing between the SM photon and the vector field  $V$  (or the hypercharge gauge boson and the weak gauge boson).

We now introduce three methods to calculate the total decay width of the dark photon  $A'$ , assuming that  $A'$  is the lightest particle in the dark sector and that a single decay channel into a fermion pair dominates its width,  $A' \rightarrow f\bar{f}$ .

### “Classical” method

First, we calculate the width in the mass basis of the vector fields, i.e., in the “classical” method. After the field redefinition (5), one obtains interactions of the dark photon in this basis as follows:

$$\mathcal{L}_{\text{int}} = (C_{VA'} g_V + C_{AA'} e Q_f) A'_\mu \bar{f} \gamma^\mu f + (C_{VV} g_V + C_{AV} e Q_f) V_\mu \bar{f} \gamma^\mu f + C_{AA} e Q_f A_\mu \bar{f} \gamma^\mu f . \quad (6)$$

Here,  $C_{IJ}$  denotes the element of the mixing matrix  $C$  in Eq. (5). Then, we obtain the decay rate of the dark photon into a pair of the fermions  $f\bar{f}$  at tree level, assuming  $f$  is a massless particle, as

$$\Gamma(A' \rightarrow f\bar{f}) = \frac{m_{A'}}{16\pi} \frac{4}{3} (g_f^{A'})^2 , \quad g_f^{A'} \equiv C_{VA'} g_V + C_{AA'} e Q_f \quad (7)$$

In the following discussion,  $g_f^I$  denotes the coupling of  $f$  to the vector field  $I$  in the mass basis. When we consider the limit of a tiny mixing parameter ( $|\eta| \ll 1$ ), a tiny kinetic mixing related to  $V$  and  $A$ ,

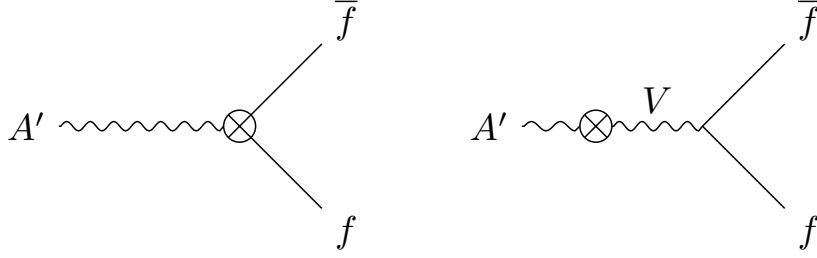


Figure 1: **Left:**  $A'$  decay via the kinetic mixing. **Right:**  $A'$  decay via the insertion of the mass mixing.

and  $\delta \rightarrow 1 - 0^+$  with  $0^+$  being a tiny positive number, the mass mixing approaches to the maximal one,  $\theta \simeq -\pi/4$ . In this limit, the mixing matrix  $C_{\text{kin}}$  approaches to the unit matrix, and one obtains  $C_{VA'} \simeq -1/\sqrt{2}$  and  $C_{AA'} \simeq 0$  at  $\mathcal{O}(\eta^0)$ . Meanwhile, for the  $V$  decay, the mixing-matrix elements are approximately  $C_{VV} \simeq 1/\sqrt{2}$  and  $C_{AV} \simeq 0$  in the limit. Therefore, the decay rates of  $A'$  and  $V$  are identical in this limit as

$$\Gamma(A' \rightarrow f\bar{f}) \simeq \Gamma(V \rightarrow f\bar{f}) \simeq \frac{m_{A'}}{16\pi} \frac{2}{3} g_V^2. \quad (8)$$

### “Mass-insertion” method

Next, we regard the mass mixing in Eq. (2) as a perturbation parameter. We calculate the decay rate in the basis where the kinetic terms are diagonalized but the mass matrix is not diagonalized. Two diagrams contribute to the  $A'$  decay, as shown in Fig. 1. One is from the direct coupling of  $A'$  to  $f\bar{f}$  after diagonalizing (canonicalizing) the kinetic term (left panel). The other is from the  $A'$ - $V$  mass mixing and propagating  $V$  as an intermediate state (right panel). Then, the decay rate is calculated as

$$\Gamma^{\text{MI}}(A' \rightarrow \bar{f}f) = \frac{M_{A'}}{16\pi^2} \frac{4}{3} \left| \bar{g}_f^{A'} + \bar{g}_f^V \frac{-\bar{m}_V^2 \eta}{M_{A'}^2 - \bar{m}_V^2 + i\bar{m}_V \bar{\Gamma}_V} \right|^2, \quad (9)$$

$$\bar{g}_f^{A'} \equiv (C_{\text{kin}})_{VA'} g_V + (C_{\text{kin}})_{AA'} eQ_f, \quad \bar{g}_f^V \equiv (C_{\text{kin}})_{VV} g_V + (C_{\text{kin}})_{AV} eQ_f,$$

where  $C_{\text{kin}}$  denotes the diagonalizing matrix for the kinetic mixing term and  $M_{A'}^2 = \bar{m}_V^2(\delta^2 + \eta^2)$ , while  $\bar{\Gamma}_V$  denotes the total decay rate of the particle  $V$  in the absence of mixing with  $A'$ :

$$\bar{\Gamma}_V = \frac{\bar{m}_V}{16\pi} \frac{4}{3} g_V^2. \quad (10)$$

We refer to this result for the decay rate of the dark photon as that of the “mass-insertion” method.  $\bar{g}_f^I$  denotes the coupling of  $f$  to the vector field  $I$  in the basis with remaining the mass mixing. We consider the same limit as that used in the above “classical” method, i.e., the limit of tiny kinetic mixing parameters and  $\delta \rightarrow 1 - 0^+$ . In this limit, the mixing matrix  $C_{\text{kin}}$  approaches the unit matrix, and its off-diagonal elements are proportional to the kinetic mixing related to  $V$  and  $A$ . Therefore, the decay rate is proportional to the square of the kinetic mixing parameters in the limit.

### Pole method

The result of the “mass-insertion” method seems inconsistent with that of the “classical” method at  $\delta \rightarrow 1$ . In the small mixing limit, the “mass-insertion” method is expected to be a good approximation

for the decay rate since the mixing parameter can be regarded as a perturbative parameter. On the other hand, from the mass-insertion term in Eq. (9), we see that it is no longer valid to treat the mass insertion perturbatively when  $|\eta| \gtrsim \bar{\Gamma}_V/\bar{m}_V$  at the limit of  $\delta \rightarrow 1$ . In such a case, the “classical” method seems to provide a good approximation to calculate the decay rate. To clarify this problem, we consider the total decay rate given by the imaginary part of the propagator pole. The particles  $V$  and  $A'$  appear as intermediate states in scattering processes such as  $f\bar{f} \rightarrow f\bar{f}$ . These are mixed with each other in the presence of quantum corrections since  $f$  couples to both  $V$  and  $A'$ . We denote the one-particle irreducible (1PI) vacuum polarizations involving the vector fields  $X$  and  $Y$  as

$$\Pi_{\mu\nu}^{IJ}(p^2) = \left( g_{\mu\nu} - \frac{p_\mu p_\nu}{p^2} \right) \Pi_{IJ}(p^2) + \frac{p_\mu p_\nu}{p^2} \Delta_{IJ}(p^2), \quad (11)$$

where  $p^\mu$  is the four-momentum of the vector fields. We drop the  $\Delta_{IJ}$  term in our analysis because only the first term contributes to the gauge-independent part of the corrections. The 1PI corrected propagators are obtained by solving the Dyson equations in the  $I$ - $J$  system shown in Fig. 2. We denote the 1PI corrected propagator involving  $I$  and  $J$  as  $-iD_{IJ}$ , where the equations are

$$\begin{aligned} -iD_{XX}(s) &= \frac{-i}{s - m_X^2} [1 + i\Pi_{XX}(s)(-iD_{XX}(s)) + i\Pi_{XY}(s)(-iD_{YX}(s))] , \\ -iD_{XY}(s) &= \frac{-i}{s - m_X^2} [0 + i\Pi_{XX}(s)(-iD_{XY}(s)) + i\Pi_{XY}(s)(-iD_{YY}(s))] , \\ -iD_{YY}(s) &= \frac{-i}{s - m_Y^2} [1 + i\Pi_{XY}(s)(-iD_{XY}(s)) + i\Pi_{YY}(s)(-iD_{YY}(s))] , \end{aligned} \quad (12)$$

where  $s = p^2$ , and  $m_{XY}^2$  denotes the mass eigenvalues in Eq. (3). Solving the equations gives

$$\begin{aligned} D_{XX}(s) &= \frac{1}{s - m_X^2 - \Pi_{XX}(s) - \frac{(\Pi_{XY}(s))^2}{s - m_Y^2 - \Pi_{YY}(s)}}, \\ D_{YY}(s) &= \frac{1}{s - m_Y^2 - \Pi_{YY}(s) - \frac{(\Pi_{XY}(s))^2}{s - m_X^2 - \Pi_{XX}(s)}}, \\ D_{XY}(s) &= \frac{\Pi_{XY}(s)}{(s - m_Y^2 - \Pi_{YY}(s))(s - m_X^2 - \Pi_{XX}(s)) - (\Pi_{XY}(s))^2}. \end{aligned} \quad (13)$$

All of these propagators have poles at the same positions in a complex  $s$  plane, which satisfies

$$[s - m_X^2 - \Pi^{XX}(s)][s - m_Y^2 - \Pi^{YY}(s)] - [\Pi^{XY}(s)]^2 = 0. \quad (14)$$

Since the vacuum polarizations are generally complex-valued, pole positions are also complex-valued. The vacuum polarizations have the form of  $\Pi_{IJ}(s) = s\Pi'_{IJ}(0)$ , ( $I, J = X, Y$ ) at the one-loop level (up to the logarithmic dependence of the real part, which we ignore as discussed later), assuming  $f$  is a massless fermion. Here, the prime ‘ $\prime$ ’ denotes a derivative with respect to the variable  $s$ . In this case, we can solve the above equation for the pole positions and find two solutions as follows:

$$\begin{aligned} s_{\text{pole}}^\pm &= \frac{1}{2} \frac{1}{(1 - \Pi'_{YY})(1 - \Pi'_{XX}) - (\Pi'_{XY})^2} \left\{ m_Y^2(1 - \Pi'_{XX}) + m_X^2(1 - \Pi'_{YY}) \right. \\ &\quad \left. \pm \sqrt{[m_Y^2(1 - \Pi'_{XX}) - m_X^2(1 - \Pi'_{YY})]^2 + 4m_Y^2 m_X^2 (\Pi'_{XY})^2} \right\}. \end{aligned} \quad (15)$$

$$\begin{aligned}
\text{X-X propagator with shaded blob} &= \text{X-X propagator with white blob} + \text{X-X propagator with white blob in middle} + \text{X-X propagator with white blob in middle} \\
\text{X-Y propagator with shaded blob} &= \text{X-Y propagator with white blob in middle} + \text{X-Y propagator with white blob in middle} + \text{X-Y propagator with white blob in middle} \\
\text{Y-Y propagator with shaded blob} &= \text{Y-Y propagator with white blob} + \text{Y-Y propagator with white blob in middle} + \text{Y-Y propagator with white blob in middle}
\end{aligned}$$

Figure 2: The Dyson equations for the  $X$ - $X$ ,  $X$ - $Y$ , and  $Y$ - $Y$  propagators. Here, a propagator with a shaded blob depicts the corresponding 1PI-corrected propagator, while a white blob shows the 1PI correction.

The real part of the pole rigorously defines the mass of the vector field, which is close to its tree-level value  $m_{V,A'}^2$  in a weak interacting theory such as the one we discuss in this article. This is why we ignore the real part of the vacuum polarization. The imaginary part of the pole gives the product of the mass and the total decay rate.

Here, we consider again the same limit used in the previous two methods: tiny kinetic mixing parameters and  $\delta \rightarrow 1 - 0^+$ . In this limit, as we saw in the first (“classical”) method, the couplings of  $X$  and  $Y$  to  $f\bar{f}$  have the same magnitude but the opposite sign, and hence one obtains  $\Pi'_{XX} \simeq \Pi'_{YY} \simeq -\Pi'_{XY} = \mathcal{O}(\eta^0)$ . We write them as  $\Pi'$  in the following discussion. The mass eigenvalues are close to each other in this limit (i.e.,  $m_X^2 \simeq m_Y^2$ ), and the mass difference is proportional to  $\eta$ . Then, when the mass difference ( $\simeq \eta \bar{m}_V^2$ ) is negligible compared to the vacuum polarization  $\Pi'$ , the poles are approximately obtained at the order of  $\eta^0$  as

$$s_{\text{pole}}^{\pm} \simeq m_X^2 (1 + \Pi' \pm \Pi') . \quad (16)$$

Thus, one of the imaginary parts of the poles is given by  $2m_X^2 \text{Im}\Pi'$ , i.e., at the order of  $\eta^0$ , while the other one is, at least, given at the order of  $\eta^2$ . Meanwhile, when the mass difference dominates the value inside of the square root, the poles are approximately given at the order of  $\eta^0$  as,

$$s_{\text{pole}}^{\pm} \simeq m_X^2 (1 + \Pi') . \quad (17)$$

In this case, the imaginary parts of the poles, namely the decay rates of the two vector fields, become identical. The poles  $s_{\text{pole}}^{\pm}$  provide the behavior of the decay rate expected by the approximate two methods. One of the mass eigenstates has the total decay rate entirely suppressed at  $\delta \rightarrow 1 - 0^+$  when  $|\eta| \lesssim |\Pi'| \simeq \bar{\Gamma}_V / \bar{m}_V$ , while the decay rates of the eigenstates are identical when  $|\eta| \gtrsim \bar{\Gamma}_V / \bar{m}_V$ . Note that even in this discussion the real part of  $\Pi$  does not play a significant role, since it does not contribute to the mass difference in the square root and suppressed by  $\pi$  compared to the imaginary part.

The particle identification of the poles might be confusing at  $\delta \simeq 1$ . The pole  $s_{\text{pole}}^+$  corresponds to  $V$  at  $\delta \ll 1$ , while it corresponds to  $A'$  at  $\delta \gg 1$ . Generally, there is a gap of order of  $\eta$  between the real parts of the poles at  $\delta \simeq 1$ . Therefore, when we define the poles  $s_{\text{pole}}^V$  and  $s_{\text{pole}}^{A'}$  being those of  $V$  and  $A'$  as above, their real parts have a discontinuity at  $\delta \simeq 1$  as a function of  $\delta$ . Meanwhile, the imaginary parts of the poles must be connected even at  $\delta \simeq 1$ : The decay rates of  $V$  and  $A'$  are identical at large  $|\eta|$ , while the decay rate of  $A'$  is suppressed at small  $|\eta|$ . In the following, we define  $s_{\text{pole}}^{A'}$  such that its imaginary part is continuously connected to what is suppressed by  $\eta^2$  apart from  $\delta \simeq 1$ .

### 3 Dark photon decay on vector resonance

We discuss in this section the three methods to calculate the decay rate of the mediator particle (i.e., “classical”, “mass-insertion”, and “pole” methods) in more detail using concrete examples of the degenerate partner. As expected, we will quantitatively see that when the mediator particle degenerates with an SM particle in mass, the “classical” and “mass-insertion” methods provide different decay rates and find that the total decay rate is well approximated by the “classical” method when  $|\eta| \gtrsim \bar{\Gamma}_V/\bar{m}_V$ , while by the “mass-insertion” method when  $|\eta| \lesssim \bar{\Gamma}_V/\bar{m}_V$ . This criterion is explicitly demonstrated by considering several degenerate partners, such as the  $Z$  boson, the  $\rho$  meson, and the true muonium. These are indeed good examples of the degenerate partner having a broad decay width (the  $\rho$  meson, which has  $\bar{\Gamma}_\rho/\bar{m}_\rho \simeq 0.2$ ), a narrow decay width (the true muonium, which has  $\bar{\Gamma}_V/\bar{m}_V \simeq 10^{-12}$ ), and an intermediate decay width (the  $Z$  boson, which has  $\bar{\Gamma}_Z/\bar{m}_Z \simeq 0.03$ ).

#### 3.1 Dark photon degenerate with the $Z$ boson

First, we consider the dark photon degenerate with the  $Z$  boson. The Lagrangian is given by Eq. (1), and canonical kinetic terms are obtained by the following redefinition of the gauge fields:

$$\begin{aligned} A'_\mu &\rightarrow \frac{1}{(1 - \epsilon^2/\cos^2 \theta_W)^{1/2}} A'_\mu, \\ Z_\mu &\rightarrow Z_\mu - \frac{\epsilon \tan \theta_W}{(1 - \epsilon^2/\cos^2 \theta_W)^{1/2}} A'_\mu, \\ A_\mu &\rightarrow A_\mu + \frac{\epsilon}{(1 - \epsilon^2/\cos^2 \theta_W)^{1/2}} A'_\mu. \end{aligned} \tag{18}$$

Here,  $\theta_W$  is the Weinberg angle, again. The mixing matrix for diagonalizing the kinetic terms of the vector fields is therefore given by

$$C_{\text{kin}} = \begin{pmatrix} \frac{1}{(1 - \epsilon^2/\cos^2 \theta_W)^{1/2}} & 0 & 0 \\ -\frac{\epsilon \tan \theta_W}{(1 - \epsilon^2/\cos^2 \theta_W)^{1/2}} & 1 & 0 \\ \frac{\epsilon}{(1 - \epsilon^2/\cos^2 \theta_W)^{1/2}} & 0 & 1 \end{pmatrix}. \tag{19}$$

Here, one obtains the mass matrix parameters  $\eta$  and  $\delta$ , which are defined in Eq. (2), as follows:

$$\eta = \frac{\epsilon \tan \theta_W}{(1 - \epsilon^2/\cos^2 \theta_W)^{1/2}}, \quad \delta = \frac{\bar{m}_{A'}/\bar{m}_Z}{(1 - \epsilon^2/\cos^2 \theta_W)^{1/2}}. \tag{20}$$

The  $Z$  boson decays into the SM fermions except for the top quark. The vector coupling of the  $Z$  boson to a fermion  $f$  is  $g_f = g_Z(T_{3f} - 2Q_f \sin^2 \theta_W)$ , while the axial-vector coupling is  $g_{5f} = g_Z T_{3f}$ . Here,  $g_Z = g/(2\cos \theta_W)$ ,  $T_{3f}$  is the weak isospin, and  $Q_f$  is the electromagnetic charge. Using  $\sin^2 \theta_W = 0.22$ , the fine structure constant of  $\alpha^{-1} = 128$ , and  $\bar{m}_Z = 91.19 \text{ GeV}$ , we obtain the SM prediction of the  $Z$  boson decay width as  $\bar{\Gamma}_Z \simeq 2.4 \text{ GeV}$ , assuming  $f$  is a massless fermion. The



decay rate of the dark photon  $A'$  using the “classical” method is given by

$$\Gamma_{A'} = \frac{m_{A'}}{16\pi} \frac{4}{3} \sum_f \left[ (g_f^{A'})^2 + (g_{5f}^{A'})^2 \right], \quad (21)$$

$$g_f^{A'} = C_{ZA'} g_f + C_{AA'} eQ_f, \quad g_{5f}^{A'} = C_{ZA'} g_{5f}.$$

Here,  $m_{A'}$  is the mass eigenvalue given in Eq. (3). As mentioned in the previous section, the above decay rate approaches  $\bar{\Gamma}_Z/2$  at  $\delta \rightarrow 1$ , as the mixing matrix element approaches  $C_{ZA'} \simeq -1/\sqrt{2}$ . Meanwhile, the coupling of the dark photon  $A'$  to the SM fermion through mixing with the  $Z$  boson is proportional to the matrix element  $C_{ZA'}$ , which is approximated at  $\eta \ll |1 - \delta^2|$  as

$$C_{ZA'} = (C_{\text{kin}})_{ZA'} \cos \theta - \sin \theta \simeq -\eta - \left( \frac{-\eta}{1 - \delta^2} \right). \quad (22)$$

It is found that the  $A'$  coupling through mixing with the  $Z$  boson,  $C_{ZA'}$ , is suppressed at  $\delta \simeq 0$ . As seen in Section 3.3 and Appendix A, it happens at a different  $\delta$  in other examples, e.g.,  $\delta \sim 1$ .

The decay rate of the dark photon  $A'$  using the “mass-insertion” method is

$$\Gamma_{A'}^{\text{MI}} = \frac{M_{A'}}{16\pi^2} \frac{4}{3} \sum_f (|\bar{g}_f|^2 + |\bar{g}_{5f}|^2), \quad (23)$$

$$\bar{g}_f = \bar{g}_f^{A'} + \bar{g}_f^Z \frac{-\eta \bar{m}_Z^2}{M_{A'}^2 - \bar{m}_Z^2 + i\bar{m}_Z \bar{\Gamma}_Z}, \quad \bar{g}_{5f} = \bar{g}_{5f}^{A'} + \bar{g}_{5f}^Z \frac{-\eta \bar{m}_Z^2}{M_{A'}^2 - \bar{m}_Z^2 + i\bar{m}_Z \bar{\Gamma}_Z}.$$

Here,  $M_{A'}^2 = \bar{m}_Z^2(\delta^2 + \eta^2)$ , and  $\bar{\Gamma}_Z$  is the decay rate of the SM  $Z$  boson in the absence of  $A'$ ,

$$\bar{\Gamma}_Z = \frac{\bar{m}_V}{16\pi} \frac{4}{3} \sum_f (g_f^2 + g_{5f}^2). \quad (24)$$

The vector and axial-vector couplings to the  $Z$  boson and the dark photon in the basis with the mass mixing are

$$\begin{aligned} \bar{g}_f^{A'} &\equiv (C_{\text{kin}})_{ZA'} g_f + (C_{\text{kin}})_{AA'} eQ_f, & \bar{g}_f^Z &\equiv (C_{\text{kin}})_{ZZ} g_f + (C_{\text{kin}})_{AZ} eQ_f, \\ \bar{g}_{5f}^{A'} &\equiv (C_{\text{kin}})_{ZA'} g_{5f}, & \bar{g}_{5f}^Z &\equiv (C_{\text{kin}})_{ZZ} g_{5f}. \end{aligned} \quad (25)$$

Since the mass-insertion contribution cancels with the contribution from the direct coupling as  $M_{A'}^2 \rightarrow 0$ , contributions from the  $Z$ -boson couplings  $g_{5f}$  are suppressed. We find similar behavior in the “classical” method, but the cancellation gets gentle because of the presence of the imaginary part  $i\bar{m}_Z \bar{\Gamma}_Z$ . The “mass-insertion” method is expected to be no longer valid as  $|\eta| \simeq |\epsilon| \gtrsim \bar{\Gamma}_Z/\bar{m}_Z \simeq 0.03$ .

The vacuum polarization rigorously determines the total decay rate in terms of the propagator pole. The imaginary part of the vacuum polarization involving the vector fields  $I$  and  $J$  is

$$\text{Im}\Pi_{IJ}(s) = -\frac{\pi}{16\pi^2} \frac{4}{3} s \sum_f (g_f^I g_f^J + g_{5f}^I g_{5f}^J), \quad (26)$$

where  $g_f^I$  and  $g_{5f}^I$  are vector and axial-vector couplings of the fermion  $f$  to the vector field  $I$  in the mass basis. Fig. 3 shows the parametric plots of the real and imaginary parts of the pole as a function

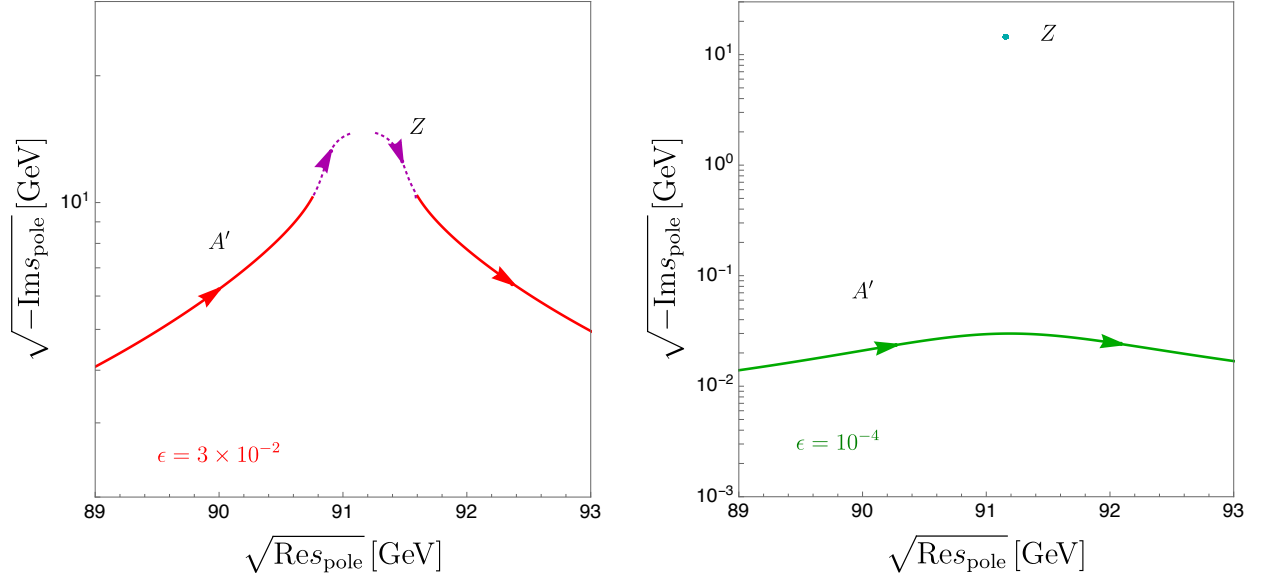


Figure 3: *Parametric plots of the real and imaginary parts of the propagator poles as a function of the parameter  $\epsilon \in [0.95, 1.05]$ , with  $\epsilon$  being fixed to be  $3 \times 10^{-2}$  (left panel) and  $10^{-4}$  (right panel), respectively.*

of the parameter  $\delta$ . The real part of the  $Z$  pole changes from  $\bar{m}_Z^2(1 + \eta)$  to  $\bar{m}_Z^2(1 - \eta)$  along the change of  $\delta \in [0.95, 1.05]$ , while the real part of the  $A'$  pole is proportional to  $\delta^2$ . The imaginary parts of both the poles are identical near  $\delta = 1$  when  $\epsilon = 3 \times 10^{-2}$  (left panel). Meanwhile, when  $\epsilon = 10^{-4}$  (right panel), the  $Z$  pole is almost unchanged, while the imaginary part of the  $A'$  pole enhances at  $\delta \simeq 1$ . Note that the real part of the pole will receive a correction from the real part of the vacuum polarization, which we ignore. We focus on the imaginary part in the followings.

The decay rate computed by the three methods is depicted in Fig. 4 as a function of  $\delta$ , with several choices of  $\epsilon$ . The right panel is a closer look at the decay rate at  $\delta \sim 1$ , and the color code and the line type are the same as the left one. First, it is seen from the figure that the three methods give the same rate except for the region of  $\delta \sim 1$ . Next, when the mass difference  $|1 - \delta|$  is smaller than  $\bar{\Gamma}_Z/\bar{m}_Z \simeq 3 \times 10^{-2}$ , the result of the “classical” method (denoted by dot-dashed lines) is not compatible with that of the “mass-insertion” method (denoted by dashed lines). Third, the result of the “mass-insertion” method agrees with the decay rate obtained by the imaginary part of the pole method (denoted by solid lines) when  $\epsilon$  is sufficiently small. On the other hand, the result of the “classical” method does not agree with the rate obtained by the pole method because it approaches  $\bar{\Gamma}_Z/2$  at  $\delta \simeq 1$  in the “classical” method. When  $\epsilon$  becomes larger than  $\bar{\Gamma}_Z/\bar{m}_Z$ , as expected from the discussion in the previous section, the result of the “mass-insertion” method is no longer in agreement with that obtained by the pole, which is seen in the lines for  $\epsilon = 3 \times 10^{-2}$ .

We also show in Fig. 5 the comparison of the decay widths obtained by the three methods as a function of  $\epsilon$ , with  $\delta$  being fixed to be one. It is seen from the figure that the decay width obtained by the “mass-insertion” method accurately reproduces the width obtained by the imaginary part of the propagator pole when  $|\epsilon| \lesssim \bar{\Gamma}_Z/\bar{m}_Z$ . On the other hand, the decay width obtained by the “classical” method accurately reproduces the width obtained by the propagator pole when  $|\epsilon| \gtrsim \bar{\Gamma}_Z/\bar{m}_Z$ .

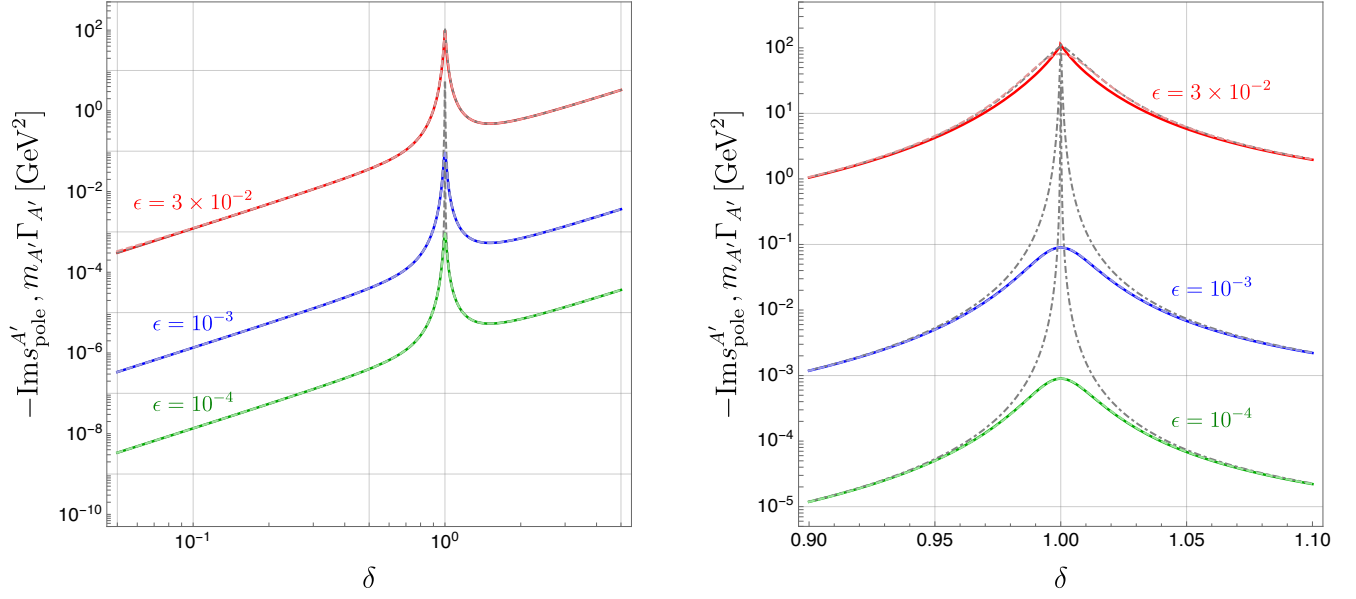


Figure 4: **Left:** The  $A'$  decay rates calculated the three methods for various values of  $\epsilon$ : the imaginary part of the propagator pole (colored solid lines), the “mass-insertion” method (colored dashed lines), and the “classical” method (gray dot-dashed lines). **Right:** A closer look at the decay rates near  $\delta = 1$ .

### 3.2 Dark photon degenerate with the $\rho$ meson

Next, we consider the dark photon degenerate with the  $\rho$  meson, one of vector hadronic resonances. We introduce the vector meson as a gauge boson of the hidden local symmetry [21]. (See Ref. [22] for a review.) The low-energy Lagrangian of the two-flavor QCD is given as follows:

$$\begin{aligned} \mathcal{L} = & -\frac{1}{4}F_{\mu\nu}F^{\mu\nu} - \frac{1}{4}F'_{\mu\nu}F'^{\mu\nu} - \frac{1}{4}V_{\mu\nu}^a V^{a\mu\nu} + \frac{\epsilon}{2}F'_{\mu\nu}F^{\mu\nu} - \frac{e}{g}\text{tr}(QV_{\mu\nu})F^{\mu\nu} \\ & + \frac{1}{2}\tilde{m}_{A'}^2 A'_\mu A'^\mu + \frac{1}{2}\tilde{m}_\rho^2 V_\mu^a V^{a\mu} + \mathcal{L}_{\text{int}} + \dots \end{aligned} \quad (27)$$

Here,  $e$  is the electromagnetic coupling, and  $g$  is the hadronic coupling. Interaction terms among the  $\rho$  meson field (i.e.,  $V_\mu = V_\mu^a t^a$  with  $t^a$  being the  $SU(2)$  generator) and pseudo-Nambu-Goldstone boson (pions) are included in  $\mathcal{L}_{\text{int}}$ . The charge matrix  $Q$  and the vector meson matrix  $V_\mu$  are given as follows:

$$Q = \frac{1}{3} \begin{pmatrix} 2 & \\ & -1 \end{pmatrix}, \quad V_\mu = \frac{1}{2} \begin{pmatrix} \rho_\mu^0 & \sqrt{2}\rho_\mu^+ \\ \sqrt{2}\rho_\mu^- & -\rho_\mu^0 \end{pmatrix}. \quad (28)$$

As the Lagrangian shows, the SM photon kinematically mixes with both the dark photon and the neutral  $\rho$  meson. There are several ways to redefine the vector fields to have canonically normalized forms.<sup>1</sup> Here, we first remove all the kinetic mixing terms by the shift:  $A_\mu \rightarrow A_\mu + \epsilon A'_\mu - (e/g)\rho_\mu^0$ . This field redefinition allows us to use the same parametrization discussed in the previous section.

<sup>1</sup>The kinetic mixing between the  $\rho$  meson and the photon is removed by shifting the  $\rho$  meson field in a conventional vector meson dominance. The photon couples to the hadronic current only through mixing with  $\rho$  for such a case.

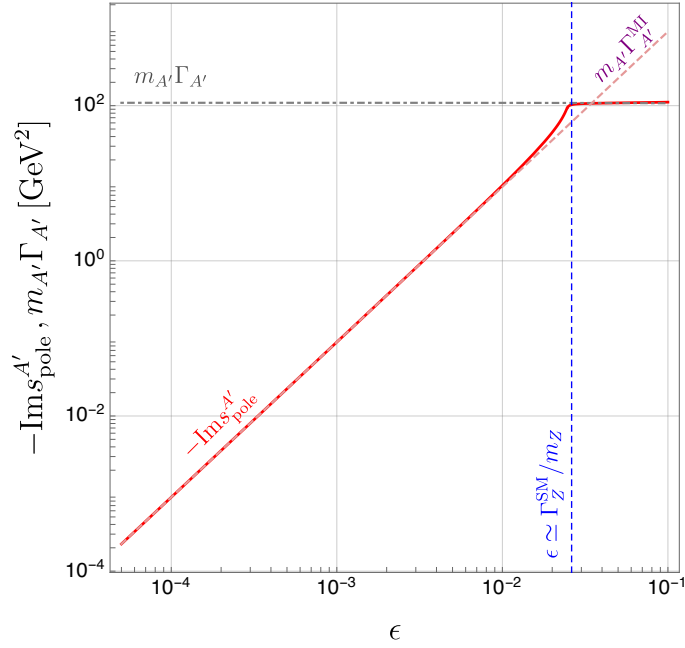


Figure 5: The decay rates of the dark photon  $A'$  degenerate with  $Z$  in mass calculated in the three methods as a function of  $\epsilon$  with  $\delta = 1$ : the imaginary part of the propagator pole (red solid line), the “mass-insertion” method (magenta dashed line), and the “classical” method (gray dot-dashed line). The blue-dashed vertical line indicates the boundary where the “mass-insertion” method is no longer valid.

After this shift, there will be the kinetic mixing between the neutral  $\rho$  meson and the dark photon. By taking the canonical normalization for the vector fields on this basis, one obtains

$$\mathcal{L} = -\frac{1}{4}F_{\mu\nu}F^{\mu\nu} - \frac{1}{4}F'_{\mu\nu}F'^{\mu\nu} - \frac{1}{4}\rho_{\mu\nu}^0\rho^{0\mu\nu} - \frac{\epsilon_{\text{eff}}}{2}\rho_{\mu\nu}^0F'^{\mu\nu} + \frac{1}{2}\bar{m}_{A'}^2 A'_\mu A'^\mu + \frac{1}{2}\bar{m}_\rho^2 \rho_\mu^0 \rho^{0\mu} + \mathcal{L}_{\text{int}} + \dots \quad (29)$$

Here,  $\bar{m}_{A'}^2 = \tilde{m}_{A'}^2/(1 - \epsilon^2)$  and  $\bar{m}_\rho^2 = \tilde{m}_\rho^2/(1 - e^2/g^2)$ . The kinetic mixing term between the neutral  $\rho$  meson and the dark photon is given by the product of two kinetic mixing factors as follows:

$$\epsilon_{\text{eff}} = \frac{\epsilon}{(1 - \epsilon^2)^{1/2}} \frac{e/g}{(1 - e^2/g^2)^{1/2}}. \quad (30)$$

This kinetic mixing term is removed by the shift  $\rho_\mu^0 \rightarrow \rho_\mu^0 + \epsilon_{\text{eff}} A'_\mu$  and subsequent rescaling. We use the same parametrization used in the mass matrix (2) for the case discussed here. Then, the parameters  $\eta$  and  $\delta$  are given

$$\eta = \frac{\epsilon_{\text{eff}}}{(1 - \epsilon_{\text{eff}}^2)^{1/2}}, \quad \delta = \frac{\bar{m}_{A'}/\bar{m}_\rho}{(1 - \epsilon_{\text{eff}}^2)^{1/2}}. \quad (31)$$

One obtains the mixing matrix, which diagonalizes all the kinetic terms of the vector fields  $(A', \rho, A)$  as

$$C_{\text{kin}} = \begin{pmatrix} \frac{1}{(1 - \epsilon_{\text{eff}}^2)^{1/2}} \frac{1}{(1 - \epsilon^2)^{1/2}} & 0 & 0 \\ -\frac{\epsilon_{\text{eff}}}{(1 - \epsilon_{\text{eff}}^2)^{1/2}} \frac{1}{(1 - e^2/g^2)^{1/2}} & \frac{1}{(1 - e^2/g^2)^{1/2}} & 0 \\ \frac{1}{(1 - \epsilon_{\text{eff}}^2)^{1/2}} \frac{\epsilon}{(1 - \epsilon^2)^{1/2}} + \frac{\epsilon_{\text{eff}}}{(1 - \epsilon_{\text{eff}}^2)^{1/2}} \frac{e/g}{(1 - e^2/g^2)^{1/2}} & -\frac{e/g}{(1 - e^2/g^2)^{1/2}} & 1 \end{pmatrix}. \quad (32)$$

The  $\rho$  meson predominantly decays into  $\pi^+\pi^-$ , so we focus only on this channel.<sup>2</sup> Then, interactions among the vector fields and the pion fields in the interaction basis are given by

$$\mathcal{L}_{\text{int}} \supset -i(eA_\mu + g\rho_\mu^0) [\pi^+(\partial^\mu \pi^-) - (\partial^\mu \pi^+)\pi^-] + (eA_\mu + g\rho_\mu^0)^2 \pi^+ \pi^-. \quad (33)$$

One obtains interaction terms in the mass basis using the mixing matrix  $C$  in Eq. (5), where it is given by the product of Eq. (32) and the one diagonalizing the mass matrix described by the parameters in Eq. (31). The decay rate of the  $\rho$  meson in the absence of  $A'$  is calculated at the tree-level as

$$\bar{\Gamma}_\rho = \frac{\bar{m}_\rho}{16\pi} \frac{1}{3} g^2. \quad (34)$$

Here, we assume that pions are massless in the final state. Choosing phenomenological favorable values  $g = 5.92$  and  $\bar{m}_\rho = 775.26$  MeV, one obtains the numerical value of  $\bar{\Gamma}_\rho$  being about 180 MeV.

Now, we calculate the decay widths of the dark photon using the three methods introduced in Section 2. The decay rate in the “classical” method, i.e., the decay rate in the mass basis, is

$$\Gamma_{A'} = \frac{m_{A'}}{16\pi} \frac{1}{3} (g_\pi^{A'})^2, \quad g_\pi^{A'} = C_{\rho A'} g + C_{AA'} e. \quad (35)$$

Meanwhile, the decay rate in the “mass-insertion” method is obtained in the basis where the mass mixing between the  $\rho$  meson and the dark photon  $A'$  remains after removing the kinetic mixing term in Eq. (29). There are two contributions to the  $A'$  decay, from the direct coupling of  $A'$  and from the mass mixing between  $\rho$  and  $A'$ . The decay width in this method is obtained as

$$\Gamma_{A'}^{\text{MI}} = \frac{M_{A'}}{16\pi} \frac{1}{3} \left| \bar{g}_\pi^{A'} + \bar{g}_\pi^\rho \frac{-\eta \bar{m}_\rho^2}{M_{A'}^2 - \bar{m}_\rho^2 + i\bar{m}_\rho \bar{\Gamma}_\rho} \right|^2, \quad (36)$$

$$\bar{g}_\pi^{A'} \equiv (C_{\text{kin}})_{\rho A'} g + (C_{\text{kin}})_{AA'} e, \quad \bar{g}_\pi^\rho \equiv (C_{\text{kin}})_{\rho\rho} g + (C_{\text{kin}})_{A\rho} e.$$

Here,  $M_{A'}^2 = \bar{m}_\rho^2(\delta^2 + \eta^2)$ . Since the interaction terms of the vector bosons have a structure similar to the standard vector meson dominance, it leads to  $\bar{g}_\pi^{A'} = 0$ . In contrast to the  $Z$  boson case, there is no cancellation between the direct and the mass-insertion contributions. Hence, the decay rate is suppressed in two limits; the decay rate is proportional to  $M_{A'}$  at small  $M_{A'}$ , while it is proportional to  $M_{A'}^{-3}$  at large  $M_{A'}$ . The “mass-insertion” method is expected to be valid at  $|\eta| \lesssim \bar{\Gamma}_\rho/\bar{m}_\rho \simeq 0.2$ .

---

<sup>2</sup>We also consider a hypothetical situation in Appendix A that  $\rho$  decays only into  $e^-e^+$ . In such a case, the decay width is suppressed at  $\mathcal{O}(1)$  keV, and it can be used to verify our discussion in a different property of the vector fields.

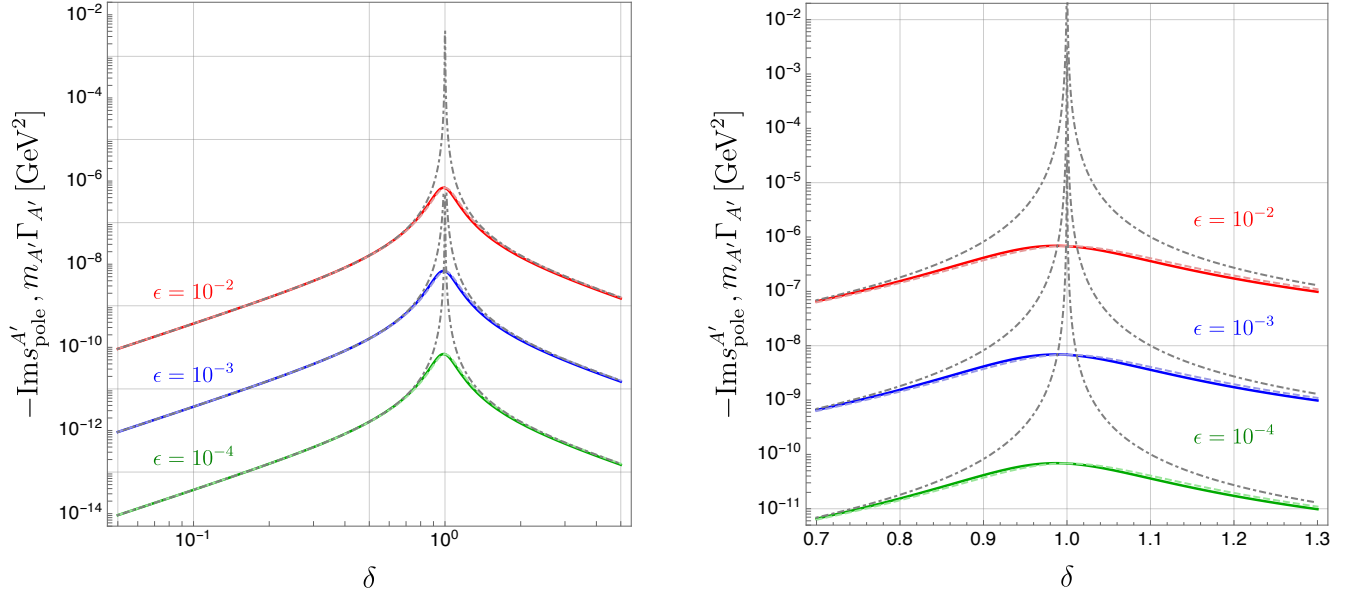


Figure 6: The same as Fig. 4, but for  $A'$  degenerate with  $\rho$  in mass. Each line code is the same as in Fig. 4. **Left:** The decay rates as a function of  $\delta$  with fixed  $\epsilon$ . **Right:** A closer look at the rates at  $\delta \simeq 1$ .

Next, we calculate the decay width of the dark photon using the vacuum polarization of the propagators for the vector fields  $X$  and  $Y$  at the one-loop level. There are two contributions to the vacuum polarization: one is from the three-point vertices  $X\pi\pi$  and  $Y\pi\pi$ , and the other is from the four-point vertices, such as  $XY\pi\pi$ . The imaginary part of the vacuum polarization is obtained as

$$\text{Im}\Pi_{IJ}(s) = -\frac{\pi s}{16\pi^2} \frac{1}{3} g_\pi^I g_\pi^J, \quad (37)$$

where  $g_\pi^I$  denotes the gauge coupling constant of the pions with regard to  $I$  in the mass basis.

Figs. 6 and 7 compares the decay rates obtained by the three methods, as those in Figs. 4 and 5. We plot the decay rates as a function of  $\delta$  in Fig. 6 for given  $\epsilon = 10^{-2}$ ,  $10^{-3}$ , and  $10^{-4}$ , while the decay rates as a function of  $\epsilon$  in Fig. 7 with  $\delta$  being fixed to be one. We use the same line types as those in Figs. 4 and 5. First, as in the previous  $Z$  boson case, the decay widths obtained by the three methods agree with each other except for the  $\delta \sim 1$  region, and the decay width obtained by the “classical” method deviates from the others in the region of  $|\delta - 1| \lesssim \bar{\Gamma}_\rho/\bar{m}_\rho$ . Next, contrary to the  $Z$  boson case, the decay rates are suppressed at large  $\delta$ . The dark photon  $A'$  does not directly couple to the pion current after diagonalizing the kinetic mixing between the  $\rho$  meson and  $A'$ . In other words,  $A'$  couples to the pion current only via the mass mixing with  $\rho$ . Therefore, the  $A'$  coupling in the mass basis is suppressed by the mixing angle  $\theta$  defined in Eq. (3) at large  $\delta$ . Finally, as seen in Fig. 7, the “classical” method is not consistent with the other methods at  $\delta \simeq 1$  even for  $\epsilon \sim 10^{-1}$ . The kinetic mixing between  $A'$  and  $\rho$  is given by the product of  $\epsilon$  and  $e/g$ , hence the criteria  $|\eta| \lesssim \bar{\Gamma}_\rho/\bar{m}_\rho$  for the validity of the use of the “mass-insertion” method implies that  $|\epsilon| \lesssim \bar{\Gamma}_\rho/\bar{m}_\rho \times (e/g)^{-1} \simeq 4$ . As far as the kinetic mixing parameter is perturbative, the result of the “mass-insertion” method always precisely approximates the decay width obtained by the imaginary part of the propagator pole.

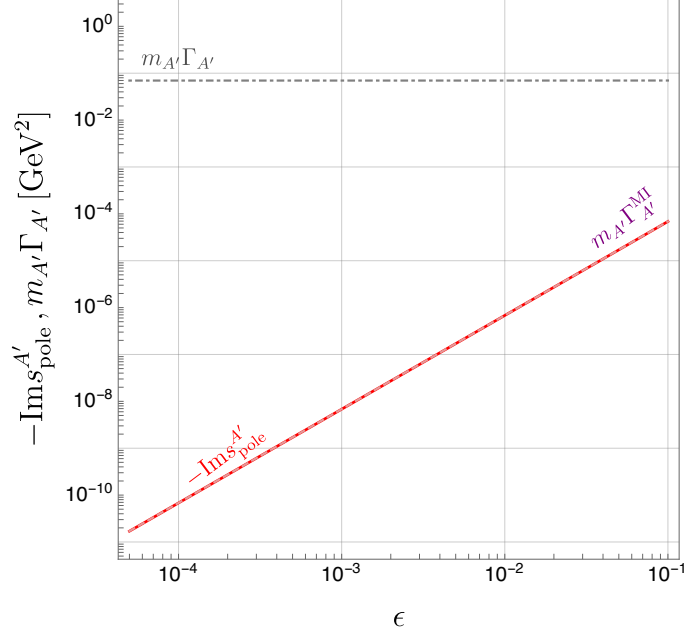


Figure 7: The same as Fig. 5, but for  $A'$  degenerate with  $\rho$  in mass. Each line code is the same as before.

### 3.3 Dark photon degenerate with the true muonium

In this subsection, as the last example to demonstrate how well our criteria work, we discuss the case with the dark photon  $A'$  degenerate with the true muonium in mass. The true muonium is the bound state composed of a muon and an antimuon.<sup>3</sup> Since the true muonium constructed with the total spin of  $S = 1$  and the orbital angular momentum of  $L = 0$  has the quantum numbers of  $J^{PC} = 1^{--}$ , the dark photon mixes with the true muonium when its mass is around the muon threshold, i.e., the twice the muon mass. We will focus on the mixing between the dark photon and the ground state of the true muonium, which we refer to as “true muonium” in the following discussion. The low energy effective Lagrangian that describes interactions among the SM photon  $A_\mu$ , the “true muonium”  $V_\mu$ , and the dark photon  $A'_\mu$  is given as follows:

$$\begin{aligned} \mathcal{L} = & -\frac{1}{4}F_{\mu\nu}F^{\mu\nu} - \frac{1}{4}F'_{\mu\nu}F'^{\mu\nu} - \frac{1}{4}V_{\mu\nu}V^{\mu\nu} + \frac{\epsilon}{2}F_{\mu\nu}F'^{\mu\nu} - \frac{\kappa}{2}F_{\mu\nu}V^{\mu\nu} \\ & + \frac{1}{2}\tilde{m}_{A'}^2 A'_\mu A'^\mu + \frac{1}{2}\tilde{m}_V^2 V_\mu V^\mu + eA_\mu J_{\text{EM}}^\mu + \dots, \end{aligned} \quad (38)$$

where  $\tilde{m}_V = 2m_\mu - \alpha^2 m_\mu/4$  is the mass parameter of the “true muonium”. The effective Lagrangian Eq. (38) is derived from the original Lagrangian Eq. (1) using the so-called potential non-relativistic (NR) Lagrangian method: it is obtained from the original Lagrangian by the NR expansion of the muon field, integrating out a soft photon field, and introducing an auxiliary field describing the “true muonium” [23]. We introduce the kinetic mixing term between the SM photon and the “true muonium” to make the gauge invariance of the Lagrangian manifest instead of the

<sup>3</sup>The positronium is also a bound state with the same quantum numbers as  $A'$ ; it decays into three photons at the one-loop level. We consider the true muonium to simplify the discussion, which decays into  $e^-e^+$  at the tree level.

mass mixing term between them. The NR method gives the mixing parameter  $\kappa = \alpha^2/2$ , which is also obtained through the consistency of the “true muonium” decay width in the absence of  $A'$ ,  $\bar{\Gamma}_V \simeq \alpha^5 m_\mu/6$ .<sup>4</sup>

Now, we calculate the decay rates of the dark photon using the three methods discussed in Section 2. Similarly to the previous examples, i.e., the  $Z$  boson and the  $\rho$  meson cases, we first calculate the mixing matrix  $C$  among the vector fields defined in Eq. (5): removing all kinetic mixing terms from the Lagrangian (38) by shifting the SM photon field as  $A_\mu \rightarrow A_\mu + \epsilon A'_\mu - \alpha^2 V_\mu/2$ , and rescaling the dark photon and the “true muonium” as  $A'_\mu \rightarrow A'_\mu/(1-\epsilon^2)^{1/2}$  and  $V_\mu \rightarrow V_\mu/(1-\alpha^4/4)^{1/2}$  to make their kinetic terms canonical. Then, we arrive at the Lagrangian,

$$\begin{aligned} \mathcal{L} = & -\frac{1}{4}F_{\mu\nu}F^{\mu\nu} - \frac{1}{4}F'_{\mu\nu}F'^{\mu\nu} - \frac{1}{4}V_{\mu\nu}V^{\mu\nu} - \frac{\epsilon_{\text{eff}}}{2}F'_{\mu\nu}V^{\mu\nu} \\ & + \frac{1}{2}\bar{m}_{A'}^2 A'_\mu A'^\mu + \frac{1}{2}\bar{m}_V^2 V_\mu V^\mu + eA_\mu J_{\text{EM}}^\mu + \epsilon eA'_\mu J_{\text{EM}}^\mu - \frac{e\alpha^2}{2}V_\mu J_{\text{EM}}^\mu + \dots \end{aligned} \quad (39)$$

Here, we introduced rescaled mass parameters  $\bar{m}_{A'} = \tilde{m}_{A'}/(1-\epsilon^2)^{1/2}$  and  $\bar{m}_V = \tilde{m}_V/(1-\alpha^4/4)^{1/2}$ . There appears a new kinetic mixing term between the dark photon and the “true muonium” with the mixing parameter,

$$\epsilon_{\text{eff}} = \frac{\epsilon}{(1-\epsilon^2)^{1/2}} \frac{\alpha^2/2}{(1-\alpha^4/4)^{1/2}}. \quad (40)$$

Further performing the shift  $V_\mu \rightarrow V_\mu - \epsilon_{\text{eff}} A'_\mu$  for the “true muonium” field and rescaling the dark photon field as  $A'_\mu \rightarrow A'_\mu/(1-\epsilon_{\text{eff}}^2)^{1/2}$ , we finally remove all kinetic mixing terms from the Lagrangian. Then, we obtain the mixing matrix  $C_{\text{kin}}$  for diagonalizing the kinetic terms of  $(A', V, A)$  as

$$C_{\text{kin}} = \begin{pmatrix} \frac{1}{(1-\epsilon_{\text{eff}}^2)^{1/2}} \frac{1}{(1-\epsilon^2)^{1/2}} & 0 & 0 \\ -\frac{\epsilon_{\text{eff}}}{(1-\epsilon_{\text{eff}}^2)^{1/2}} \frac{1}{(1-\alpha^4/4)^{1/2}} & \frac{1}{(1-\alpha^4/4)^{1/2}} & 0 \\ \frac{1}{(1-\epsilon_{\text{eff}}^2)^{1/2}} \frac{\epsilon}{(1-\epsilon^2)^{1/2}} + \frac{\epsilon_{\text{eff}}}{(1-\epsilon_{\text{eff}}^2)^{1/2}} \frac{\alpha^2/2}{(1-\alpha^4/4)^{1/2}} & -\frac{\alpha^2/2}{(1-\alpha^4/4)^{1/2}} & 1 \end{pmatrix}, \quad (41)$$

Combining this and the mass mixing matrix between  $V$  and  $A'$ , we obtain the mixing matrix  $C$  relating the interaction basis with the mass basis, as seen in Eq. (5). The mass mixing parameters in the mass matrix (3) normalized by the mass of the “true muonium”,  $\eta$  and  $\delta$ , are given as

$$\eta = \frac{\epsilon_{\text{eff}}}{(1-\epsilon_{\text{eff}}^2)^{1/2}}, \quad \delta = \frac{\bar{m}_{A'}/\bar{m}_V}{(1-\epsilon_{\text{eff}}^2)^{1/2}}. \quad (42)$$

Using the mixing matrices  $C$  and  $C_{\text{kin}}$  in Eq. (41), the decay widths of the dark photon  $A'$ , which are calculated using the “classical” and the “mass-insertion” methods, are obtained as follows:

$$\Gamma_{A'} = \frac{\alpha m_{A'}}{3} |C_{AA'}|^2, \quad \Gamma_{A'}^{\text{MI}} = \frac{\alpha M_{A'}}{3} \left| (C_{\text{kin}})_{AA'} + (C_{\text{kin}})_{AV} \frac{-\bar{m}_V^2 \eta}{M_{A'}^2 - \bar{m}_V^2 + i\bar{m}_V \bar{\Gamma}_V} \right|^2, \quad (43)$$

---

<sup>4</sup>We include only the contribution from the  $\mu^- \mu^+$  pair annihilation into  $e^- e^+$  inside the true muonium and ignore the contribution from the decay of the component particles  $\mu^-$  and  $\mu^+$ . This is because the latter contribution,  $\Gamma_\mu \simeq 2.99 \times 10^{-16}$  MeV, is much smaller than the former one  $\bar{\Gamma}_V \simeq 3.66 \times 10^{-10}$  MeV. See Appendix B for details.



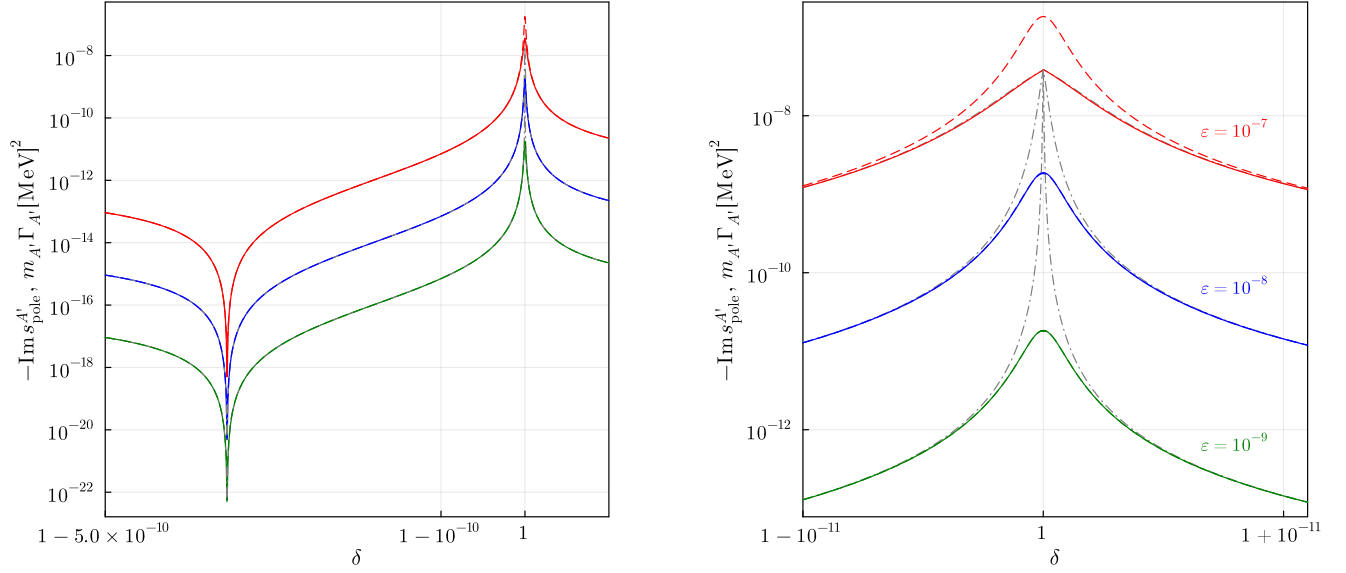


Figure 8: *The same as Figs. 4 and 6, but for the dark photon  $A'$  degenerate with the “true muonium” in mass. Each line code is also the same as those in Figs. 4 and 6. **Left:** The decay rates as a function of  $\delta$  with  $\epsilon$  begin fixed to be several values. **Right:** A closer look at the rates with  $\delta$  being fixed to be one.*

respectively. Here,  $M_{A'}^2 = \bar{m}_V^2(\eta^2 + \delta^2)$  is the mass of the dark photon in the bases with the mass mixing term. In addition, with  $I, J$  representing the vector fields  $X, Y$  in the mass basis, i.e., the dark photon and the “true muonium”, we also obtain the imaginary part of the vacuum polarization, which is required to calculate the decay width in the pole method, as follows:

$$\text{Im}\Pi_{IJ}(s) = -\frac{\alpha}{3}sC_{AI}C_{AJ}. \quad (44)$$

Fig. 8 compares the decay widths of the dark photon as a function of  $\delta$  with fixed  $\epsilon$  ( $10^{-7}$ ,  $10^{-8}$ , and  $10^{-9}$ ) calculated using the three methods. We use the same line types as the previous subsections: colored solid lines for the pole method, colored dashed lines for the “mass-insertion” method, and gray dot-dashed lines for the “classical” method. One can observe that, excluding the region of  $\delta \simeq 1$  (the maximum mixing  $m_{A'} \simeq m_V$ ), the three methods yield the decay widths in good agreement. However, in the vicinity of  $\delta = 1$ , the “classical” method approximates the pole method when  $\epsilon = 10^{-7}$ , while the “mass-insertion” method gives the widths compatible with those of the pole method when  $\epsilon$  is smaller, i.e.,  $\epsilon = 10^{-8}$  and  $10^{-9}$ . This observation is more readily confirmed by examining each width as a function of  $\epsilon$  with  $\delta$  fixed to be one, as illustrated in the left panel of Fig. 9. For the “true muonium” case, the kinetic mixing  $\epsilon_{\text{cr}}$  that saturates the criteria  $|\eta| \sim \bar{\Gamma}_V/\bar{m}_V$  is approximately given by  $\epsilon_{\text{cr}} \simeq 3.2 \times 10^{-8}$  according to Eqs. (40) and (42), and thus the “classical” method breaks down as  $|\epsilon| > \epsilon_{\text{cr}}$ .

There exists a sharp dip in the decay rates around  $\delta \simeq (1 - \alpha^4/4)^{1/2}$  apart from the  $|\delta - 1| \lesssim \bar{\Gamma}_V/\bar{m}_V$  region as seen in the left panel of Fig. 8 (see also the right panel of Fig. 9 for a closer look). In the “classical” method, the decay rate  $\Gamma_{A'}$  in Eq. (43) becomes zero when the two contributions to  $C_{AA'}$ , i.e., the decay directly from the dark photon and that via the “true muonium”, cancel each other out. The “mass-insertion” method also involves two contributions to  $\Gamma_{A'}^{\text{MI}}$ . However, the complete cancellation does not occur due to the imaginary part present in the propagator of the

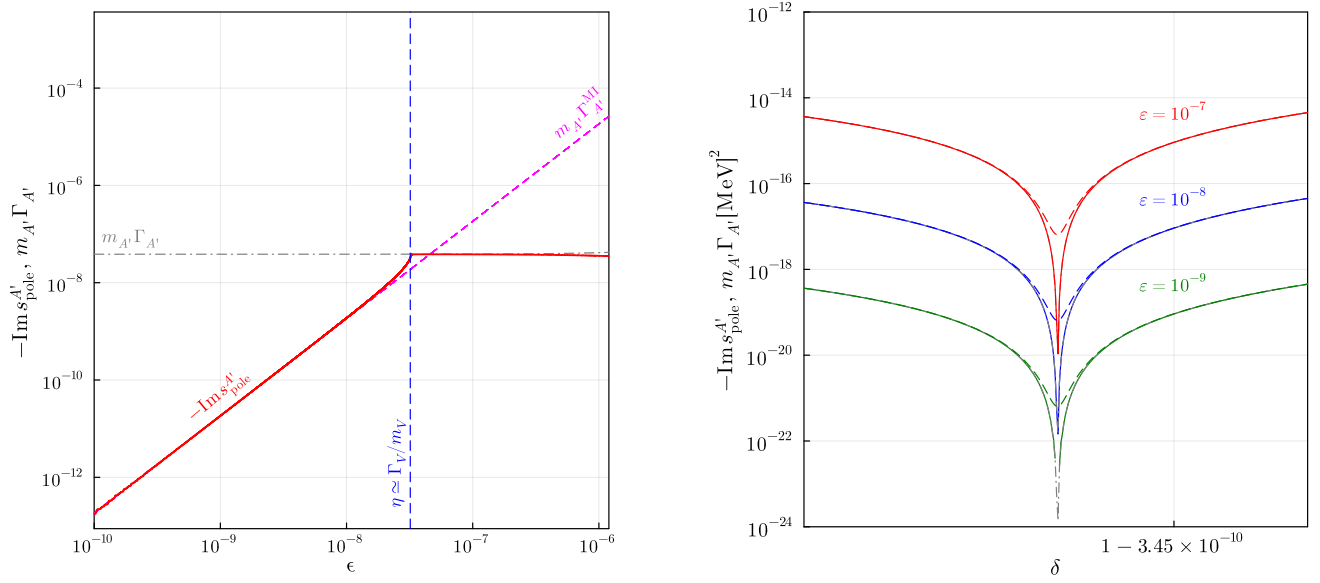


Figure 9: **Left:** The same as Figs. 5 and 7, but for  $A'$  degenerate with the “true muonium” in mass. Each line code is the same as in Figs. 5 and 7. **Right:** A closer look at the rates near the destructive interference.

“true muonium”, and the destructive interference is smeared compared to that of the “classical” decay width  $\Gamma_{A'}$ . The decay width obtained in the pole method exhibits destructive interference similar to the “classical” decay width. This fact can be understood by examining the denominator of  $D_{A'A'}$  in Eq. (13).  $C_{AA'} = 0$  when the destructive interference occurs. Since both vacuum polarizations  $\Pi_{A'A'}$  and  $\Pi_{A'V}$  included in the denominator of  $D_{A'A'}$  vanish, the decay width in the pole method gets zero.

## 4 Summary and application

Taking the dark photon as an example of a mediator particle connecting the SM and the dark sectors, we introduced the three methods to calculate the decay width of the mediator particle in Section 2. Then, it is found that the decay widths obtained in these methods behave differently when the mediator particle and the SM partner are (nearly-)degenerate in mass in the interaction basis.

### “Classical” method

The decay width of the mediator particle is calculated at tree level in the mass basis, where the field redefinition removes all kinetic and mass mixing among fields relevant to the discussion.

### “Mass-insertion” method

We take the basis where the field redefinition removes all kinetic mixing terms while the mass mixing term remains. Regarding the mass mixing between the dark photon and the SM field as a small perturbative parameter, we calculate the decay width by inserting it once.

### Pole method

Imaginary parts of poles found in current-current correlation functions provide the decay widths of intermediate states, i.e., the mediator particle and its degenerate partner. We obtain the widths by calculating vacuum polarizations in the mass basis and resumming them.

In the “classical” method, the dark photon strongly mixes with the SM degenerate partner even if the kinetic mixing parameter  $\epsilon$  between their fields is small. As a result, the dark photon has a width comparable to that of the degenerate partner. To be more precise, the widths of the two particles become almost half the width the degenerate partner in the absence of  $A'$ . Note that this fact does not lead to an immediate inconsistency with observations. At first glance, halving the width of the degenerate partner also changes the prediction of the production cross-section for its resonance search. However, the dark photons are simultaneously produced with the same quantum numbers (and in almost the same amount) as one of the intermediate states of the process, and the total event rate does not change. To discriminate the two signals, one from the mediator particle and the other from the degenerate partner, we need the energy resolution to discriminate a tiny mass difference between them. Meanwhile, the decay width of the dark photon using the “mass-insertion” method is explicitly suppressed by the mass mixing; thus, the dark photon gets long-lived as the kinetic mixing is very small. A key feature of the “mass-insertion” method is treating the mass mixing perturbatively, as discussed in Section 2. However, when the mass mixing is comparable to the decay rate of the degenerate partner, namely  $|\eta| \gtrsim \bar{\Gamma}_V/\bar{m}_V$ , the mass mixing is no longer treated as a perturbative parameter (and it requires the resummation of diagrams with multiple insertions of the mass mixing). In such a case, the decay width of the dark photon using the “classical” method correctly reproduces the rigorous one, i.e., the decay width using the pole method.

**Our criterion**  $|\eta| \simeq \bar{\Gamma}_V/\bar{m}_V$

In Section 3, to demonstrate that our criterion for the approximated methods works, in the scenarios with degenerate partners  $Z$ ,  $\rho$ , and “true muonium”, we made a numerical comparison among the decay widths of the dark photon using the three methods, assuming that the pole method gives correct decay widths. Then, we found the followings: (i) when the mass of the dark photon is far away from that of the degenerate partner, the decay widths using the three methods are in good agreement. (ii) when the mass difference is comparable to the decay widths of the partner particles, the “classical” method and the “mass-insertion” method yield different decay rates. The “mass-insertion” method agrees well with the pole method when  $|\eta| \lesssim \bar{\Gamma}_V/\bar{m}_V$ , whereas the “classical” method does when  $|\eta| \gtrsim \bar{\Gamma}_V/\bar{m}_V$ . This criterion is expected to be universal (as far as low-energy interactions are written in terms of effective field theories); it depends only on the decay rate normalized by its mass and not on other properties of the degenerate partner, e.g., it does not rely on whether the partner is a fundamental particle, a resonance, or a bound state.

## Application to other resonances

Let us now consider a general case where the dark photon degenerate with a vector meson. We introduce the critical value of the kinetic mixing parameter between the SM photon and the dark photon, denoted by  $\epsilon_{\text{cr}}$ : the “classical” (“mass-insertion”) method gives the correct decay rate when the mixing parameter is larger (smaller) than it. To determine  $\epsilon_{\text{cr}}$ , it is necessary to know the mass mixing parameter  $\eta$  between the dark photon and the meson. Assuming the vector meson is described by the massive vector field, low-energy interaction terms among the SM photon, the vector meson

$H$ , and the dark photon are given by

$$\begin{aligned}\mathcal{L} = & -\frac{1}{4}F_{\mu\nu}F^{\mu\nu} - \frac{1}{4}H_{\mu\nu}H^{\mu\nu} - \frac{1}{4}F'_{\mu\nu}F'^{\mu\nu} + \frac{\epsilon}{2}F_{\mu\nu}F'^{\mu\nu} - \frac{\epsilon_H}{2}F_{\mu\nu}H^{\mu\nu} \\ & + \frac{1}{2}m_H^2 H_\mu H^\mu + \frac{1}{2}m_{A'}^2 A'_\mu A'^\mu + eA_\mu J_{\text{EM}}^\mu + \cdots,\end{aligned}\quad (45)$$

where  $H_{\mu\nu} = \partial_\mu H_\nu - \partial_\nu H_\mu$  and  $\tilde{m}_H$  are the field strength tensor and the mass of  $H$ , respectively. Here, we assume that (i) the dark photon interacts with the SM through the kinetic mixing between the SM photon and the dark photon, (ii) the meson  $H$  interacts with the SM leptons through one photon exchange<sup>5</sup> and its coupling is controlled by the kinetic mixing parameter  $\epsilon_H$  between the SM photon and the meson.<sup>6</sup> Following the same discussion as in the previous section, the non-diagonal element of the mass matrix  $\eta$  is obtained after removing all the kinetic mixing terms as

$$\eta = \frac{\epsilon}{(1 - \epsilon^2)^{1/2}} \frac{\epsilon_H}{(1 - \epsilon_H^2)^{1/2}}. \quad (46)$$

The vector meson  $H$  decays into  $e^-e^+$  through the mixing parameter  $\epsilon_H$  with the decay rate,

$$\Gamma(H \rightarrow e^-e^+) = \frac{\bar{m}_H}{16\pi} \frac{4}{3} \epsilon_H^2 e^2, \quad (47)$$

where  $\bar{m}_H^2 = \tilde{m}_H^2/(1 - \epsilon_H^2)$ . Using the branching ratio of the vector meson  $H$  decaying to a pair of an electron and a positron,  $\text{Br}(H \rightarrow e^-e^+)$ , and the total decay width of the vector meson  $\bar{\Gamma}_H$ , the unknown parameter  $\epsilon_H$  can be written as follows:

$$\epsilon_H = \left[ \frac{3 \text{Br}(H \rightarrow e^-e^+) \bar{\Gamma}_H / \bar{m}_H}{\alpha} \right]^{1/2}. \quad (48)$$

Then, the critical value of the kinetic mixing parameter,  $\epsilon_{\text{cr}}$ , which saturates the criterion  $|\eta| \simeq \bar{\Gamma}_H$  as discussed above, can be quantitatively evaluated in a general case through the following equation:<sup>7</sup>

$$\frac{\epsilon_{\text{cr}}}{(1 - \epsilon_{\text{cr}}^2)^{1/2}} \simeq \left[ \frac{\alpha \bar{\Gamma}_H / \bar{m}_H}{3 \text{Br}(H \rightarrow e^-e^+)} \right]^{1/2}. \quad (49)$$

Table 1 shows various mesons with  $J^{\text{PC}} = 1^{--}$  quantum numbers, their masses, total decay widths, branching ratios into  $e^-e^+$ , and critical values of the kinetic mixing  $\epsilon_{\text{cr}}$  estimated using Eq. (49). Light vector mesons, i.e., from  $\rho(770)$  to  $\phi(1020)$ , are composed of light  $u, d$  and  $s$  quarks, whereas heavy vector mesons, i.e., from  $J/\psi(1S)$  to  $\psi(4160)$  and from  $\Upsilon(1S)$  to  $\Upsilon(11020)$ , predominantly made up of  $c\bar{c}$  and  $b\bar{b}$  quarks, respectively. For vector mesons whose dominant decay modes are hadronic and are not suppressed by the Okubo-Zweig-Iizuka (OZI) rule [?, ?, ?], such as light vector mesons, e.g.,  $\rho(770)$ ,  $\omega(782)$ , and  $\phi(1020)$ , and heavy quarkonia, e.g.,  $\psi(3770)$  and

<sup>5</sup>Multiple photon exchanges are also possible to consider. However, those processes are higher-order corrections to the one photon exchanged diagram in QED. Our prescription used here corresponds to disregarding such corrections.

<sup>6</sup>On the contrary, in addition to the simple photon exchange mentioned above, hadronic currents  $J_{\text{Had}}^\mu$  can couple directly to the vector meson through the current interaction  $H_\mu J_{\text{Had}}^\mu$ , as is known in the vector meson dominance.

<sup>7</sup>We estimate the critical value  $\epsilon_{\text{cr}}$  using the branching fraction into a  $e^-e^+$  pair. Considering the picture of bound states composed of heavy quarkonia and the existence of other decay modes, it may be possible to estimate  $\epsilon_{\text{cr}}$  more accurately. We expect that the order of the magnitude for  $\epsilon_{\text{cr}}$  does not significantly change from our estimate.

Mesons	Mass (MeV)	Width (MeV)	Branching ratio to $e^-e^+$	Critical mixing $\epsilon_{\text{cr}}$
$\rho(770)$	775.26	149.1	$4.72 \times 10^{-5}$	$9.53 \times 10^{-1}$
$\omega(782)$	782.66	8.68	$7.38 \times 10^{-5}$	$5.26 \times 10^{-1}$
$\phi(1020)$	1019.461	4.249	$2.979 \times 10^{-4}$	$1.81 \times 10^{-1}$
$J/\psi(1S)$	3090.9	$9.26 \times 10^{-2}$	$5.971 \times 10^{-2}$	$1.10 \times 10^{-3}$
$\psi(2S)$	3686	$2.94 \times 10^{-1}$	$7.93 \times 10^{-3}$	$4.95 \times 10^{-3}$
$\psi(3770)$	3773.7	27.2	$9.6 \times 10^{-6}$	$8.04 \times 10^{-1}$
$\psi(4040)$	4039	80	$1.07 \times 10^{-5}$	$9.05 \times 10^{-1}$
$\psi(4160)$	4191	70	$6.9 \times 10^{-6}$	$9.25 \times 10^{-1}$
$\Upsilon(1S)$	9460	$5.4 \times 10^{-2}$	$2.38 \times 10^{-2}$	$7.64 \times 10^{-4}$
$\Upsilon(2S)$	10023	$3.198 \times 10^{-2}$	$1.91 \times 10^{-2}$	$6.38 \times 10^{-4}$
$\Upsilon(3S)$	10355	$2.032 \times 10^{-2}$	$2.18 \times 10^{-2}$	$4.68 \times 10^{-4}$
$\Upsilon(4S)$	10579.4	20.5	$1.57 \times 10^{-5}$	$4.81 \times 10^{-1}$
$\Upsilon(10860)$	10885.2	37	$8.3 \times 10^{-6}$	$7.67 \times 10^{-1}$
$\Upsilon(11020)$	11000	24	$5.4 \times 10^{-6}$	$7.04 \times 10^{-1}$

Table 1: Masses, total decay widths, and branching fractions into a  $e^-e^+$  pair of vector mesons that could be mixed with the dark photon  $A'$ , and the critical values of the kinetic mixing Eq. (49).

$\Upsilon(4S)$ , their total decay widths are large, so that the critical kinetic mixing  $\epsilon_{\text{cr}}$  becomes  $\mathcal{O}(1)$ . Therefore, for the kinetic mixing not excluded by experiments so far searching for the visible decay of the dark photon, the “mass-insertion” method provides an accurate prediction of the decay width of the dark photon degenerate with such a vector meson. On the other hand, for vector mesons with dominant decay modes suppressed by the OZI rule (e.g.,  $J/\psi(1S)$ ,  $\Upsilon(1S)$ ),  $\epsilon_{\text{cr}}$  is  $\mathcal{O}(10^{-3})$  or smaller, so that we have to choose the approximation method correctly, the “classical” method and the “mass-insertion” method, depending on the magnitude of  $\epsilon$ .

## 5 Concluding remarks

We consider the decay of the mediator particle in the presence of a nearly degenerate SM particle by taking the dark photon as an example. We find that the “mass-insertion” method, in which we treat the mass-mixing parameter (denoted as  $\eta$ ) perturbatively, is valid as far as  $\eta$  is smaller than the decay width of the degenerate particle normalized by its mass. The “classical” method, in which we compute the decay rate in the mass basis, overestimates the decay rate in such a case when the mass difference is smaller than about the decay width of the degenerate partner particle.

### Implication for existing literature

The “classical” method has been used for  $Z$  and  $A'$  in the literature. In the context of collider searches, including electroweak precision tests of the dark photon (or the  $Z'$  boson) [24, 25], and the thermal relic abundance of the inelastic dark matter [26–28]. In the former analysis, the  $Z$  boson mass and the couplings of the  $Z$  boson to the SM fermions are affected in the presence of the dark photon. Then, electroweak observables written in terms of the couplings and the mass are affected. When  $A'$  is degenerate with  $Z$  in mass, it is better to write the observables in terms of the cross-section with re-summed propagators because the couplings of the  $Z$  boson significantly

change (with a factor of  $1/\sqrt{2}$ ). Meanwhile, in the latter analysis, the annihilation cross-section of the inelastic dark matter into SM fermions through  $A'$  and  $Z$  is computed on the mass basis. Considering exclusively  $A'$  or  $Z$  in the mass basis, the annihilation cross-section would be artificially enhanced when  $m_{A'}^2 \simeq m_Z^2$ .

### Use of the $R$ -ratio

The hadronic decay of the dark photon  $A'$  is often estimated using a method similar to the “mass-insertion” method (e.g., see Refs. [29–32]). The dark photon couples to the electromagnetic current through kinetic mixing between the dark and SM photons. Since the theoretical evaluation of the hadron matrix element of the current-current correlation function is not feasible, it is estimated by experimental data, so-called the  $R$ -ratio,  $R(s) = \sigma(e^+e^- \rightarrow \text{hadrons}; s)/\sigma(e^+e^- \rightarrow \mu^+\mu^-; s)$ . More specifically, for the dark photon mass above the hadronic thresholds, the hadronic decay rate is evaluated as

$$\Gamma(A' \rightarrow \text{hadrons}) = R(s = m_{A'}^2) \Gamma(A' \rightarrow \mu^+\mu^-). \quad (50)$$

Here  $\Gamma(A' \rightarrow \mu^+\mu^-)$  is evaluated in the mass basis for  $Z$  and  $A'$  (not including hadronic resonances). The resultant decay rate is always suppressed by a factor of  $\epsilon^2$ , and thus  $\epsilon$  is treated perturbatively as in the “mass-insertion” method. At the same time, the impact on the  $R$ -ratio on a broad resonance peak is also suppressed by a factor of  $\epsilon^2$ . Thus the above seems a good approach near broad resonances even for moderate  $\epsilon \sim 0.1$ , for instance. On the other hand, near narrow vector resonances (e.g.,  $J/\psi(1S)$  with  $\bar{\Gamma}_H/\bar{m}_H \simeq 3 \times 10^{-5}$ , and  $\Upsilon(1S)$  with  $\bar{\Gamma}_H/\bar{m}_H \simeq 6 \times 10^{-6}$ ), this underestimates the correct decay width of the dark photon  $A'$ . In such a case, the “classical” method may provide the correct decay rate, which implies that the decay widths of the vector meson and  $A'$  are nearly equal to each other (and the half of the vector meson in the absence of  $A'$ ). As noted above, this does not immediately affect the  $R$ -ratio. The mass difference between the vector meson and  $A'$  is tiny and thus it may require a high energy resolution to resolve signal events in the experiment into those from the  $A'$  decay and those from the decay of the vector resonances.

### Future work

This study focuses on the total decay width of the mediator particles. Other quantities are also crucial for terrestrial experiments, such as the production cross-section of the mediator particles and the branching fraction into a specific final state. We should also consider the influence of the presence of the degenerate partner on these quantities and leave the dedicated analysis of them for a future study. We take the dark photon as an example of the mediator particle in Section 3. However, as discussed in Section 2, the “mass-insertion” method is expected to be valid only when the mass mixing is smaller than the decay rate (normalized by the mass) of the nearly degenerate particle  $V$  even when we consider other mediator scenarios, such as those with the dark Higgs mediator.

## Acknowledgements

A. K. acknowledges partial support from Norwegian Financial Mechanism for years 2014-2021, grant nr 2019/34/H/ST2/00707; and from National Science Centre, Poland, grant 2017/26/E/ST2/00135

and DEC-2018/31/B/ST2/02283. The work of T. K. is supported in part by the National Science Foundation of China under Grant Nos. 11675002, 11635001, 11725520, 12235001, and 12250410248. S. M. is supported by Grant-in-Aid for Scientific Research from the MEXT, Japan (20H01895, 20H00153, 19H05810, 18H05542, JPJSCCA20200002). S. M. and Yuki W. are also supported by the World Premier International Research Center Initiative(WPI), MEXT, Japan(Kavli IPMU). Yu W. is supported by JSPS KAKENHI Grant Number 23KJ0470.

## A Example: $\rho$ dominantly decaying into electrons

We discuss again the dark photon decaying through the mixing with the  $\rho$  meson discussed in Section 3. In the SM, the dominant decay mode of the  $\rho$  meson is that into a  $\pi^+\pi^-$  final state. In this appendix, we consider a hypothetical case where the  $\rho$  meson dominantly decays into a  $e^+e^-$  pair; even so, we assume the same coupling  $g = 5.92$  and the same mass  $m_\rho = 775.26 \text{ MeV}$ . The electrons couple to the vector fields only through the electromagnetic current. Hence, the  $\rho$  meson decays into a pair of electrons only through the kinetic mixing between the  $\rho$  meson and photon, and the decay rate of the  $\rho$  meson at the tree level is suppressed by the kinetic mixing,

$$\bar{\Gamma}_\rho^{ee} = \frac{m_\rho}{16\pi} \frac{4}{3} \left| \frac{e/g}{\sqrt{1 - e^2/g^2}} e \right|^2, \quad (51)$$

and numerically  $\bar{\Gamma}_\rho^{ee} = 4.96 \text{ keV}$ . This decay channel provides an example of the resonance with  $\bar{\Gamma}_\rho^{ee}/\bar{m}_\rho \simeq 6 \times 10^{-6}$ , which is between two  $\bar{\Gamma}_V/\bar{m}_V$ s for the pion channel of the  $\rho$  meson and for the “true muonium”. The decay rate of the dark photon calculated in the “classical” method is given by

$$\Gamma_{A'}^{ee} = \frac{m_{A'}}{16\pi} \frac{4}{3} |C_{AA'} e|^2. \quad (52)$$

Here, the mixing matrix  $C_{AA'}$  is given in Eqs. (5) and (32). Meanwhile, the decay rate by the “mass-insertion” method is

$$\begin{aligned} \Gamma_{A'}^{ee;\text{MI}} &= \frac{M_{A'}}{16\pi} \frac{4}{3} \left| \bar{g}_e^{A'} + \bar{g}_e^\rho \frac{-\eta \bar{m}_\rho^2}{M_{A'}^2 - \bar{m}_\rho^2 + i\bar{m}_\rho \bar{\Gamma}_{\rho e}} \right|^2, \\ \bar{g}_e^{A'} &\equiv (C_{\text{kin}})_{AA'} e, \quad \bar{g}_e^\rho \equiv (C_{\text{kin}})_{A\rho} e. \end{aligned} \quad (53)$$

Since the tree-level coupling  $\bar{g}_e^{A'}$  does not vanish in the electron channel in contrast to the pion channel, there appears a cancellation between two contributions from the direct coupling and from the mass insertion for a certain parameters. Finally, the imaginary part of the vacuum polarization from the electron loop is given by

$$\text{Im}\Pi_{IJ}(s) = -\frac{\pi s}{16\pi^2} \frac{4}{3} g_e^I g_e^J. \quad (54)$$

Here,  $g_e^I$  in the above formula denotes the coupling of the electron to the vector field  $I$ .

We show in Fig. 10 the comparison of the total decay rates calculated using the three methods. We choose two different values of  $\epsilon$ :  $\epsilon = 10^{-3}$  (red) and  $\epsilon = 10^{-5}$  (blue). As expected, the decay

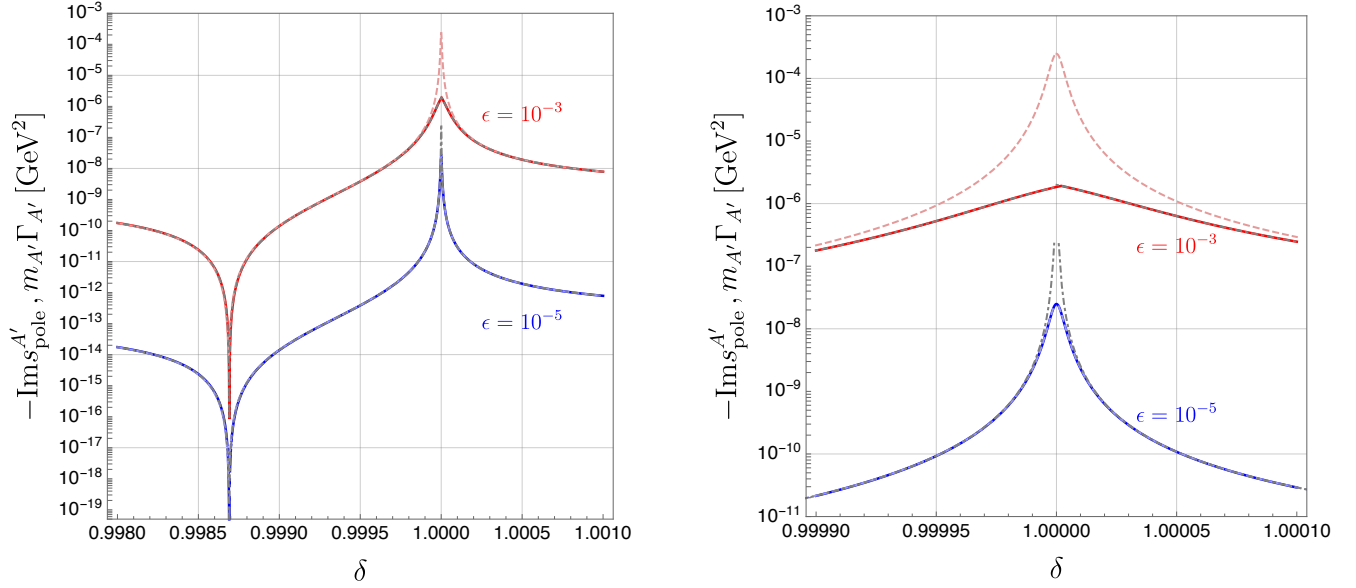


Figure 10: The same as Fig. 6, but  $A'$  decays only into  $e^+e^-$ . Each line code is the same as that in Fig. 6. **Left:** The decay rates as functions of  $\delta$  for a fixed  $\epsilon$ . **Right:** A closer look at decay rates near  $\delta = 1$ .

rates using the three methods are in agreement with each other except for the region with  $\delta \simeq 1$ . When  $\delta$  approaches to unity (within the range of  $\bar{\Gamma}_\rho^{ee}/\bar{m}_\rho \simeq 6 \times 10^{-6}$ ), the three methods are not compatible with each other. The “mass-insertion” method (depicted as colored-dashed lines) gives the width in agreement with the width by the pole method when  $|\eta| \lesssim \bar{\Gamma}_\rho^{ee}/\bar{m}_\rho$  (or  $|\epsilon| \lesssim 10^{-4}$ ). On the other hand, the “classical” method (depicted as dot-dashed lines) gives the width in agreement with the width by the pole method when  $|\eta| \gtrsim \bar{\Gamma}_\rho^{ee}/\bar{m}_\rho$  (or  $|\epsilon| \gtrsim 10^{-4}$ ). We also see a destructive interference near  $\delta \simeq 0.9987$  in the right panel of Fig. 10. Let us consider the decay width using the “mass-insertion” method in Eq. (53). Since the location of the destructive interference is enough away from  $\delta = 1$ , we can ignore the imaginary part of the propagator,  $i\bar{m}_\rho\bar{\Gamma}_\rho^{ee}$ . Then, we find the decay rate vanishes at  $\delta \simeq (1 - e^2/g^2)^{1/2} \simeq 0.9987$ .

As in Section 3, we also show the comparison of the rates as a function of  $\epsilon$  with  $\delta = 1$  in Fig. 11. When  $\epsilon$  is larger than the threshold (i.e., given by  $|\eta| \simeq \bar{\Gamma}_\rho^{ee}/\bar{m}_\rho$ ), the decay rate of  $A'$  by the imaginary part of the pole agrees with that by the “classical” method. This behavior is consistent with the conclusion in the text. A destructive behavior is again seen at  $\epsilon \simeq 0.05$ . There, the coupling of the dark photon to an electron and a positron in the mass basis,

$$C_{AA'} = \frac{e/g}{\sqrt{1 - e^2/g^2}} \cos \theta + \eta \left( \frac{e/g}{\sqrt{1 - e^2/g^2}} - \frac{\sqrt{1 - e^2/g^2}}{e/g} \right) \sin \theta, \quad (55)$$

vanishes at a specific  $\eta$  for  $\delta = 1$ , where the mass mixing is almost maximum,  $\theta \simeq +\pi/4$ . Then, we find  $\eta \simeq e^2/g^2$  (or  $\epsilon \simeq e/g \simeq 0.05$ ) by solving  $C_{AA'} = 0$ . We note that, as discussed in Section 2, the particles are identified by their decay rates near  $\delta = 1$ . The dark photon  $A'$  in mass basis corresponds to the mass eigenstate whose eigenvalue is given by  $m_Y^2$  in Eq. (3) at  $\delta$  far from unity. On the other hand, near  $\delta = 1$ , the dark photon  $A'$  corresponds to the mass eigenstate whose eigenvalue is given



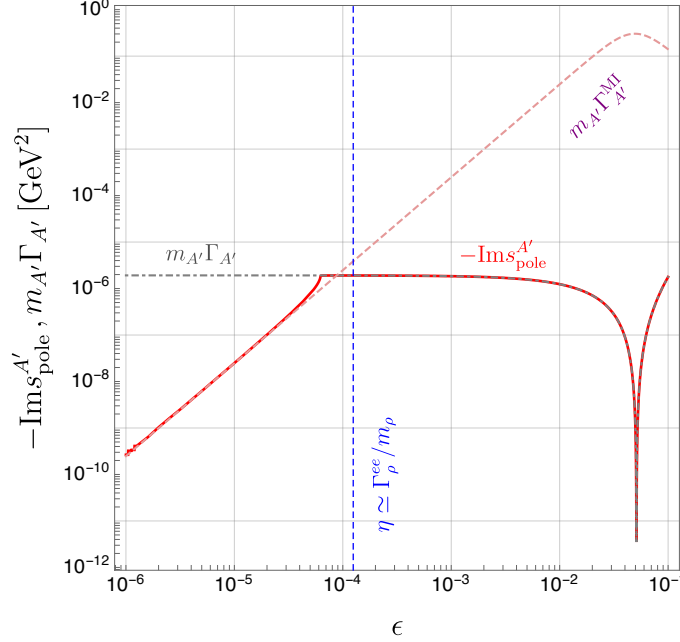


Figure 11: The same as Fig. 6, but  $A'$  decays only into  $e^+e^-$ . Each line code is the same as in Fig. 6.

by  $m_X^2$ . Therefore, at  $\delta$  far from unity, we should use the coupling,

$$C_{AA'} = -\frac{e/g}{\sqrt{1-e^2/g^2}} \sin \theta + \eta \left( \frac{e/g}{\sqrt{1-e^2/g^2}} + \frac{\sqrt{1-e^2/g^2}}{e/g} \right) \cos \theta. \quad (56)$$

## B Kinetic mixing with true muonium

We show the detail of determining the mixing parameter  $\kappa$  between the SM photon and the (ground-state) “true muonium” in the effective field theory (EFT) (42) and deriving the decay width of the “true muonium”. To obtain  $\kappa$ , we match the amplitude of the  $V \rightarrow e^-e^+$  process in QED and the EFT. First, in the QED calculation, we assume that the state of the “true muonium”, i.e., a non-relativistic bound state, can be written by a superposition of a pair of the freely moving non-relativistic  $\mu^-$  and  $\mu^+$  states as follows:

$$|V, S, S_z\rangle \simeq \sqrt{2m_V} \sum_{s_1, s_2} \sigma_{s_1 s_2}^{SS_z} \int \frac{d^3 p}{(2\pi)^3} \tilde{\psi}(\vec{p}) \frac{1}{\sqrt{2m_\mu}} |\mu^-; +\vec{p}, s_1\rangle \otimes \frac{1}{\sqrt{2m_\mu}} |\mu^+; -\vec{p}, s_2\rangle, \quad (57)$$

where  $\sigma_{s_1 s_2}^{SS_z}$  is the wave function of the spin describing the spin-triplet state, while  $\tilde{\psi}(\vec{p})$  is the Fourier transformation of the wave function  $\psi(\vec{r})$  that describes the muon-antimuon system in the position space. Note that  $\psi(\vec{r})$  is obtained by solving the Schrödinger equation with the Hamiltonian  $H = -\nabla^2/m_\mu - \alpha/r$ . Moreover,  $|\mu^- (\mu^+); \vec{p}, s\rangle$  is the state vector of the muon (antimuon) with the momentum  $\vec{p}$  and the spin  $s$ . Here, to normalize the state in a covariant way, we put a factor

$1/\sqrt{2m_\mu}$ . Using the expression of the “true muonium” in Eq. (57), we obtain the amplitude as

$$\mathcal{M}^{\text{QED}}(V \rightarrow e^- e^+) = \frac{1}{\sqrt{m_\mu}} \sum_{s_1, s_2} \sigma_{s_1 s_2}^{SS_z} \int \frac{d^3 p}{(2\pi)^3} \tilde{\psi}(\vec{p}) \mathcal{M}^{\text{QED}}[(\mu^-; +\vec{p}, s_1) (\mu^+; -\vec{p}, s_2) \rightarrow e^- e^+], \quad (58)$$

where  $\mathcal{M}^{\text{QED}}[(\mu^-; +\vec{p}, s_1) (\mu^+; -\vec{p}, s_2) \rightarrow e^- e^+]$  is the amplitude from a pair of  $\mu^-$ ,  $\mu^+$  into  $e^- e^+$  with muon-antimuon momenta and spins being  $\vec{p}$ ,  $-\vec{p}$  and  $s_1$ ,  $s_2$ , respectively. This amplitude is explicitly given by

$$\mathcal{M}^{\text{QED}}[(\mu^-; +\vec{p}, s_1) (\mu^+; -\vec{p}, s_2) \rightarrow e^- e^+] = \frac{e^2}{m_V^2} [\bar{v}_{s_2}(-\vec{p}) \gamma_\mu u_{s_1}(\vec{p})] [\bar{u}(\vec{k}) \gamma^\mu v(-\vec{k})], \quad (59)$$

with  $u(\vec{p})$  and  $v(\vec{p})$  being the spinor wave functions associated with the external lines, and  $\vec{k}$  being the momentum of the outgoing electron  $e^-$ . Remembering  $\mu^-$  and  $\mu^+$  are non-relativistic,  $u_s(\vec{p})$  and  $v_s(-\vec{p})$  becomes independent of their momenta, and the wave function part in Eq. (58) is factored out, and its value is simply given by the wave function at the origin in the position space, i.e.,  $\psi(0) = (\alpha^3 m_\mu^3 / 8\pi)^{1/2}$ . On the other hand, in the EFT, we obtain the amplitude as follows:

$$\mathcal{M}^{\text{EFT}}(V \rightarrow e^- e^+) = e \kappa \epsilon_\mu(S_z) \bar{u}(\vec{k}) \gamma^\mu v(-\vec{k}), \quad (60)$$

where  $\epsilon_\mu$  is the polarization vector of the “true muonium”. From the matching condition on Eqs. (58) and (60), we find  $\kappa = \alpha^2/2$ .<sup>8</sup> In addition, following the standard procedure from amplitude to a physical quantity, Eq. (58) gives the decay width of the “true muonium” as  $\Gamma_V = \alpha^5 m_\mu / 6$ .

## References

- [1] A. Fradette, M. Pospelov, J. Pradler, and A. Ritz, “Cosmological Constraints on Very Dark Photons,” *Phys. Rev. D* **90** no. 3, (2014) 035022, [arXiv:1407.0993 \[hep-ph\]](#).
- [2] A. Kamada and H.-B. Yu, “Coherent Propagation of PeV Neutrinos and the Dip in the Neutrino Spectrum at IceCube,” *Phys. Rev. D* **92** no. 11, (2015) 113004, [arXiv:1504.00711 \[hep-ph\]](#).
- [3] M. Hufnagel, K. Schmidt-Hoberg, and S. Wild, “BBN constraints on MeV-scale dark sectors. Part II. Electromagnetic decays,” *JCAP* **11** (2018) 032, [arXiv:1808.09324 \[hep-ph\]](#).
- [4] M. Ibe, A. Kamada, S. Kobayashi, and W. Nakano, “Composite Asymmetric Dark Matter with a Dark Photon Portal,” *JHEP* **11** (2018) 203, [arXiv:1805.06876 \[hep-ph\]](#).
- [5] M. Ibe, S. Kobayashi, Y. Nakayama, and S. Shirai, “Cosmological constraint on dark photon from  $N_{\text{eff}}$ ,” *JHEP* **04** (2020) 009, [arXiv:1912.12152 \[hep-ph\]](#).
- [6] **APEX** Collaboration, S. Abrahamyan *et al.*, “Search for a New Gauge Boson in Electron-Nucleus Fixed-Target Scattering by the APEX Experiment,” *Phys. Rev. Lett.* **107** (2011) 191804, [arXiv:1108.2750 \[hep-ex\]](#).

---

<sup>8</sup>The spinor wave functions are  $u_s(\vec{p}) \simeq \sqrt{2m_\mu}(\chi_s, 0)^T$  and  $v_s(-\vec{p}) \simeq -\sqrt{2m_\mu}(0, \chi'_s)^T$  in the Dirac representation with  $\chi_s$  and  $\chi'_s = -i\sigma^2 \chi_s$  being the two-component spinor, and  $\chi_{s=+1} = (1, 0)^T$  and  $\chi_{s=-1} = (0, 1)^T$ . The polarization vectors are  $\epsilon^\mu(S_z = 1) = -(0, 1, i, 0)/\sqrt{2}$ ,  $\epsilon^\mu(S_z = 0) = (0, 0, 0, 1)$  and  $\epsilon^\mu(S_z = -1) = (0, 1, -i, 0)/\sqrt{2}$ .

- [7] **KLOE-2** Collaboration, F. Archilli *et al.*, “Search for a vector gauge boson in  $\phi$  meson decays with the KLOE detector,” *Phys. Lett. B* **706** (2012) 251–255, [arXiv:1110.0411 \[hep-ex\]](#).
- [8] **KLOE-2** Collaboration, D. Babusci *et al.*, “Limit on the production of a light vector gauge boson in phi meson decays with the KLOE detector,” *Phys. Lett. B* **720** (2013) 111–115, [arXiv:1210.3927 \[hep-ex\]](#).
- [9] **BaBar** Collaboration, J. P. Lees *et al.*, “Search for a Dark Photon in  $e^+e^-$  Collisions at BaBar,” *Phys. Rev. Lett.* **113** no. 20, (2014) 201801, [arXiv:1406.2980 \[hep-ex\]](#).
- [10] **LHCb** Collaboration, R. Aaij *et al.*, “Search for hidden-sector bosons in  $B^0 \rightarrow K^{*0} \mu^+ \mu^-$  decays,” *Phys. Rev. Lett.* **115** no. 16, (2015) 161802, [arXiv:1508.04094 \[hep-ex\]](#).
- [11] **NA48/2** Collaboration, J. R. Batley *et al.*, “Search for the dark photon in  $\pi^0$  decays,” *Phys. Lett. B* **746** (2015) 178–185, [arXiv:1504.00607 \[hep-ex\]](#).
- [12] **LHCb** Collaboration, R. Aaij *et al.*, “Search for long-lived scalar particles in  $B^+ \rightarrow K^+ \chi(\mu^+ \mu^-)$  decays,” *Phys. Rev. D* **95** no. 7, (2017) 071101, [arXiv:1612.07818 \[hep-ex\]](#).
- [13] **LHCb** Collaboration, R. Aaij *et al.*, “Search for Dark Photons Produced in 13 TeV  $pp$  Collisions,” *Phys. Rev. Lett.* **120** no. 6, (2018) 061801, [arXiv:1710.02867 \[hep-ex\]](#).
- [14] **NA62** Collaboration, E. Cortina Gil *et al.*, “Search for  $\pi^0$  decays to invisible particles,” *JHEP* **02** (2021) 201, [arXiv:2010.07644 \[hep-ex\]](#).
- [15] **NA62** Collaboration, E. Cortina Gil *et al.*, “Measurement of the very rare  $K^+ \rightarrow \pi^+ \nu \bar{\nu}$  decay,” *JHEP* **06** (2021) 093, [arXiv:2103.15389 \[hep-ex\]](#).
- [16] **CMS** Collaboration, A. Tumasyan *et al.*, “Search for long-lived particles decaying into muon pairs in proton-proton collisions at  $\sqrt{s} = 13$  TeV collected with a dedicated high-rate data stream,” *JHEP* **04** (2022) 062, [arXiv:2112.13769 \[hep-ex\]](#).
- [17] J. L. Feng *et al.*, “The Forward Physics Facility at the High-Luminosity LHC,” *J. Phys. G* **50** no. 3, (2023) 030501, [arXiv:2203.05090 \[hep-ex\]](#).
- [18] **Belle-II** Collaboration, I. Adachi *et al.*, “Search for a long-lived spin-0 mediator in  $b \rightarrow s$  transitions at the Belle II experiment,” [arXiv:2306.02830 \[hep-ex\]](#).
- [19] **FASER** Collaboration, H. Abreu *et al.*, “Search for dark photons with the FASER detector at the LHC,” *Phys. Lett. B* **848** (2024) 138378, [arXiv:2308.05587 \[hep-ex\]](#).
- [20] B. Holdom, “Two U(1)’s and Epsilon Charge Shifts,” *Phys. Lett. B* **166** (1986) 196–198.
- [21] M. Bando, T. Kugo, S. Uehara, K. Yamawaki, and T. Yanagida, “Is rho Meson a Dynamical Gauge Boson of Hidden Local Symmetry?,” *Phys. Rev. Lett.* **54** (1985) 1215.
- [22] M. Harada and K. Yamawaki, “Hidden local symmetry at loop: A New perspective of composite gauge boson and chiral phase transition,” *Phys. Rept.* **381** (2003) 1–233, [arXiv:hep-ph/0302103](#).

- [23] S. Matsumoto, Y. Watanabe, Y. Watanabe, and G. White, “Decay of the mediator particle at threshold,” *JHEP* **09** (2023) 015, [arXiv:2212.10739 \[hep-ph\]](#).
- [24] A. Hook, E. Izaguirre, and J. G. Wacker, “Model Independent Bounds on Kinetic Mixing,” *Adv. High Energy Phys.* **2011** (2011) 859762, [arXiv:1006.0973 \[hep-ph\]](#).
- [25] D. Curtin, R. Essig, S. Gori, and J. Shelton, “Illuminating Dark Photons with High-Energy Colliders,” *JHEP* **02** (2015) 157, [arXiv:1412.0018 \[hep-ph\]](#).
- [26] E. Izaguirre, G. Krnjaic, and B. Shuve, “Discovering Inelastic Thermal-Relic Dark Matter at Colliders,” *Phys. Rev. D* **93** no. 6, (2016) 063523, [arXiv:1508.03050 \[hep-ph\]](#).
- [27] E. Izaguirre, Y. Kahn, G. Krnjaic, and M. Moschella, “Testing Light Dark Matter Coannihilation With Fixed-Target Experiments,” *Phys. Rev. D* **96** no. 5, (2017) 055007, [arXiv:1703.06881 \[hep-ph\]](#).
- [28] A. Berlin and F. Kling, “Inelastic Dark Matter at the LHC Lifetime Frontier: ATLAS, CMS, LHCb, CODEX-b, FASER, and MATHUSLA,” *Phys. Rev. D* **99** no. 1, (2019) 015021, [arXiv:1810.01879 \[hep-ph\]](#).
- [29] J. D. Bjorken, R. Essig, P. Schuster, and N. Toro, “New Fixed-Target Experiments to Search for Dark Gauge Forces,” *Phys. Rev. D* **80** (2009) 075018, [arXiv:0906.0580 \[hep-ph\]](#).
- [30] J. Blümlein and J. Brunner, “New Exclusion Limits on Dark Gauge Forces from Proton Bremsstrahlung in Beam-Dump Data,” *Phys. Lett. B* **731** (2014) 320–326, [arXiv:1311.3870 \[hep-ph\]](#).
- [31] A. Berlin, S. Gori, P. Schuster, and N. Toro, “Dark Sectors at the Fermilab SeaQuest Experiment,” *Phys. Rev. D* **98** no. 3, (2018) 035011, [arXiv:1804.00661 \[hep-ph\]](#).
- [32] P. Ilten, Y. Soreq, M. Williams, and W. Xue, “Serendipity in dark photon searches,” *JHEP* **06** (2018) 004, [arXiv:1801.04847 \[hep-ph\]](#).